

Mechanistic empirical studies of emulsion stabilized bases using finite element method

Kumar, Abhinav; Gupta, Ankit; Anupam, Kumar; Singh, Aakash; Premarathna, Saranga

DOI

[10.1080/15397734.2025.2491033](https://doi.org/10.1080/15397734.2025.2491033)

Publication date

2025

Document Version

Final published version

Published in

Mechanics Based Design of Structures and Machines

Citation (APA)

Kumar, A., Gupta, A., Anupam, K., Singh, A., & Premarathna, S. (2025). Mechanistic empirical studies of emulsion stabilized bases using finite element method. *Mechanics Based Design of Structures and Machines*, 53(10), 6863-6890. <https://doi.org/10.1080/15397734.2025.2491033>

Important note

To cite this publication, please use the final published version (if applicable).
Please check the document version above.

Copyright

Other than for strictly personal use, it is not permitted to download, forward or distribute the text or part of it, without the consent of the author(s) and/or copyright holder(s), unless the work is under an open content license such as Creative Commons.

Takedown policy

Please contact us and provide details if you believe this document breaches copyrights.
We will remove access to the work immediately and investigate your claim.

ISSN: 1539-7734 (Print) 1539-7742 (Online) Journal homepage: www.tandfonline.com/journals/lmbd20

Mechanistic empirical studies of emulsion stabilized bases using finite element method

Abhinav Kumar, Ankit Gupta, Kumar Anupam, Aakash Singh & Saranga Premarathna

To cite this article: Abhinav Kumar, Ankit Gupta, Kumar Anupam, Aakash Singh & Saranga Premarathna (15 Apr 2025): Mechanistic empirical studies of emulsion stabilized bases using finite element method, *Mechanics Based Design of Structures and Machines*, DOI: 10.1080/15397734.2025.2491033

To link to this article: <https://doi.org/10.1080/15397734.2025.2491033>




© 2025 The Author(s). Published with
license by Taylor & Francis Group, LLC



Published online: 15 Apr 2025.



Submit your article to this journal 



Article views: 597

[View related articles](#) View Crossmark data 

Mechanistic empirical studies of emulsion stabilized bases using finite element method

Abhinav Kumar^a, Ankit Gupta^a, Kumar Anupam^b, Aakash Singh^a, and Saranga Premarathna^b

^aDepartment of Civil Engineering, Indian Institute of Technology (BHU), Varanasi, India; ^bDepartment of Civil Engineering & Geoscience, Delft University of Technology, Delft, the Netherlands

ABSTRACT

Emulsion-treated aggregate base layer structure is one of the popular choices to form a more stabilized layer, in which aggregates are treated with slow-setting bitumen emulsion. The aim of the study is to propose a three-dimensional finite element model that is capable of showing the potential benefits of using an emulsion-treated aggregate layer. The damaging effect of overloading and high temperature in a tropical climatic condition on the pavement response have been highlighted in this study. The analyses showed that by using an emulsion-treated aggregate layer, the rut resistance and fatigue life considerably improve.

HIGHLIGHTS

- Resilient behavior of various mixes at different temperatures has been presented.
- Laboratory evaluation of the resilient modulus for pavement design has been highlighted.
- A FE-based tire pavement structure is developed to evaluate mechanistic response of the asphalt pavement.
- The effect of emulsion-stabilized base on the AC structural performance has been discussed.

ARTICLE HISTORY



Received 14 November 2024
Accepted 2 April 2025

KEYWORDS

Emulsion-treated aggregate; FE modeling; tire-pavement interaction; mechanical properties; structural response

1. Introduction

Asphalt concrete (AC) pavement structure are considered as mechanistically complex systems due to their composition of different materials and regular interaction with surrounding conditions (Helwany, Dyer, and Leidy 1998). Hence, their performance is influenced by parameters such as material properties, loading conditions, and environmental factors. In emerging economies like India, the surface layer of AC pavement is recognized as bituminous concrete (BC) and stone mastic asphalt (SMA) as a popular choice for pavement construction compared to open-graded friction course (OGFC) (Ghosh, Padmarekha, and Krishnan 2013). The reason could be mainly because the road construction agencies are uncertain about the reliability of OGFC (a relatively new technology in the Indian market) (Akarsh et al. 2022). The Ministry of Road Transport & Highways (MoRTH) specifications (MoRTH 2013) categorize BC based on their aggregate sizes. The first category, BC-1, is classified with a nominal aggregate size of 19 mm, whereas the second

CONTACT Kumar Anupam  k.anupam@tudelft.nl  Department of Civil Engineering & Geoscience, Delft University of Technology, Delft, The Netherlands
Communicated by Wei-Chau Xie.

© 2025 The Author(s). Published with license by Taylor & Francis Group, LLC

This is an Open Access article distributed under the terms of the Creative Commons Attribution License (<http://creativecommons.org/licenses/by/4.0/>), which permits unrestricted use, distribution, and reproduction in any medium, provided the original work is properly cited. The terms on which this article has been published allow the posting of the Accepted Manuscript in a repository by the author(s) or with their consent.

category, BC-2, is classified with a nominal aggregate size of 13.2 mm. Similar to BC, MoRTH (2013) categorizes SMA-1 with a nominal aggregate size of 13 mm and SMA-2 with a nominal aggregate size of 19 mm. These different mixes are known to exhibit relatively different mechanical properties under varying surrounding conditions. Therefore, understanding the characteristics of these mixes under applied load and environmental factors is crucial for performance-based design.

Understanding the behavior of these asphalt mixes is key to achieving the expected lifespan. Uncertainties (like material response to traffic loading subjected to different environmental conditions) during the mix design phase can lead to significant errors in lifespan estimation. To reduce the risk of early failures in asphalt pavements, Indian road agencies require these asphalt mix samples to be tested under controlled laboratory conditions. The resilient modulus (M_r) values, which represent the stiffness of the mixture, are one of the recommended parameters for performance-based design (IRC 36-2018 2018). The M_r values are obtained through the elastic recovery principle *via* indirect tensile strength (ITS) using a Dynamic Testing System setup (Karami et al. 2018). Since the Dynamic Testing System setup is expensive, it is still out of reach for many research laboratories in emerging economies like India. To address this issue, Indian Road Congress (IRC) (IRC 36-2018 2018) prescribes M_r values for BC mixes at different test temperatures, which IRC obtained based on extensive laboratory and field-testing data. However, M_r values, as suggested by several researchers (Venudharan and Biligiri 2015; Karami et al. 2018), vary significantly with the choice of ingredients and their proportions at different temperatures. Hence, IRC (IRC 36-2018 2018) recommends M_r values of BC mixes at some prescribed temperatures. However, it does not provide any recommendations for SMA mixes. In cases where either SMA is used or temperature conditions significantly differ from the specified temperatures on which M_r values of other mixes are provided by IRC (IRC 36-2018 2018), further exploration of pavement performance design evaluation is often necessary (assuming a laboratory test for M_r could not be performed).

Pavement performance design is traditionally carried out by evaluating the structural responses such as stress, strain, and deformations of the pavement system (Zhang et al. 2020). Several past literature studies (Khan et al. 2013; Gupta, Kumar, and Rastogi 2015; Ranadive and Tapase 2016) discuss the structural responses of the Indian pavement system, however, considering standard axle load on conventional unbound granular layers. Limited study on effect of base or subbase layer stabilization on pavement performance is available. As per current design practices in India, the M_r values are used as an important input parameter for the mechanical characterization of the asphalt mixes. The M_r values of SMA mixes are not available in the design guidelines, implies that the pavement responses for SMA considering M_r value is still a topic of research. Hence, in this research focus is given to develop a finite element-based framework which is capable of studying the response of pavement system considering the SMA layer also with different thermal resilient behavior considering the conventional base layer. This framework can address the challenges of material characterization, interface friction, loading, and other complicated issues related to environmental inputs which is not possible to incorporate through analytical solutions. However, other challenges related to construction activities like requirement of aggregates at large scale needs special attention in today's context (considering growing scarcity of natural sources).

In modern days, scientists are putting their effort to minimize the use of virgin natural resources (Bocci et al. 2010; Grilli et al. 2016; Chhabra, RN, and Singh 2022; Andrews, Radhakrishnan, Koshy, Chowdary, et al. 2023; Andrews, Radhakrishnan, Koshy, and Prasad 2023; Anupam et al. 2023). Since in pavement construction, good quality aggregates are required in the top layer (AC layer), saving aggregate quantity in this layer will ultimately result in reduction of natural resources. However, an immediate question is the cracking of stabilized base under repeated load and temperature variation which has not been taken into account and will be considered in future study with dense graded asphalt mixes. Researcher (Dias, Núñez, and Fedrigo 2024) in past have

studied gap-graded mixes as wearing course over a permeable cold bituminous emulsion mix to limit crack reflection. The emulsion stabilized materials have also been used as overlay to limit excessive elastic deformation and rutting (Dias et al. 2023). The actual benefit and cost analysis is beyond the scope of this article. In India, research is being carried out to develop stabilized base layer (Chhabra, RN, and Singh 2022; Andrews, Radhakrishnan, Koshy, Chowdary, et al. 2023; Andrew, Radhakrishnan, Koshy, and Prasad 2023; Shukla et al. 2023) which should effectively increase the overall strength of the structure. Base stabilization is often carried out using emulsion and active fillers (Chhabra, RN, and Singh 2022; Andrews, Radhakrishnan, Koshy, Chowdary, et al. 2023; Andrews, Radhakrishnan, Koshy, and Prasad 2023). This increase in overall strength could ultimately be utilized to reduce the thickness of the AC layer, still meeting the design requirements. Such a reduction in the thickness of the AC layer could lead to a reduction of virgin aggregates and develop more economical and sustainable design practices. Literature studies show that there has been limited research regarding the above-mentioned aspect within IRC design specifications (IRC 37-2012 2012). Hence, in this research, the proposed finite element (FE)-based framework will be utilized to understand the effect of base stabilization on the reduction of top layer thickness.

As discussed in the previous section, the use of virgin natural resources is seen as a major concern in India due to limited access and environmental related issues. Early failures of asphalt pavement often led to the utilization of these resources during reconstruction/maintenance activities. One of the major causes as identified by researchers (Pais, Amorim, and Minhoto 2013; Júnior et al. 2020; Abadin and Hayano 2022) is overloading of the pavement structure than the design loading. Although certain road agencies have adopted some measures to limit overloading, still it prevails in many road sections. An immediate approach to limit the severity of the damage could be to provide leverage in the pavement layer with minimum cost. Past literature (De Beer and Grobler 1994) concluded that, stabilized base treatment results in an increase in stiffness of about 300% during the first 10 months. An increase in layer stiffness may allow for higher tire loading as compared to the conventional base layer. This can provide limited leverage against overloaded vehicles.

As discussed in the above paragraphs, the main objective of this research is to propose a FE-based tire-pavement interaction framework which is capable of assessing the structural behavior of different pavement systems considering various mixtures and different materials for the base layer. It is noted that the proposed model is versatile which can be recalibrated to the requirements of different road research agencies of the world. The mechanical characterization of unbound granular layers is done by M_r and Poisson's ratio in the FE model as input parameters. Since, the commonly adopted circular contact area of uniform pressure distribution may not accurately reflect real field conditions, an actual solid tire was modeled at the tire-pavement interface. Recent studies (Lu et al. 2019) have explored 3D finite element model using X-ray computed tomography to study the mechanical response of asphalt pavement under real tire's stress distribution. De Beer, Fisher, and Jooste (2002) quantified several pavement response parameters using nonuniform contact stresses at different asphalt moduli. The response data were later benchmarked with multi-layered linear elastic theory. However, to the best of authors' knowledge, none of the existing studies focused on developing an FE-based framework which is capable of evaluating the impact of a stabilized base on the reduction of AC layer thickness and providing leverage for the overloading under nonuniform loading conditions.

2. Scope of the study

In order to achieve the objectives as discussed in Section 1, the following research scopes were set:

- a. A three-dimensional AC pavement and solid tire for loading have been modeled to study the mechanistic response of the pavement subjected to different loading conditions. The analysis was carried out at different tire loads of 20, 25, 30, 35, and 40 kN. The structural response of the pavement in terms of stress, strain, and deformation has been evaluated and discussed at three different test temperatures of 25, 35, and 45 °C.
- b. Four different mixes, BC-1, BC-2, SMA-1, and SMA-2 have been used to study the effect of aggregate gradation and binder content on the structural response of the AC pavement. These mixtures are popular choices in Indian road construction. The selection of test temperatures is based on the highest temperature rise during various seasons in India.
- c. A finite element-based framework has been developed that can study the effect of base layer stabilization on the critical mechanistic parameters, vertical compressive strain at the top of the subgrade (ϵ_z) and horizontal tensile strain at the bottom of the AC layer (ϵ_t). The benefits of base stabilization in terms of reduction in AC layer thickness and allowance for overloading have also been highlighted.

3. Description of the material properties

In this research, silty soil was considered as subgrade soil because it shares approximately 46% of the Indian soil landscape. The swelling index of the used soil sample was found to be 13%, which falls well within the specified maximum limit of 50% as per IS (IS 2720 – Part 40 1997). When tested in accordance with the standard (IS 2720 – Part 8 1994), the maximum dry unit weight was found to be 17.91 kN/m³, which is higher than the minimum specified limit of 17.5 kN/m³. The subsequent subsections will discuss the physical characteristics of binder and aggregates used in this research.

3.1. Properties of asphalt binders

In the present research, a viscosity graded binder, VG-40 was used with an absolute viscosity of 4480 Poise at 60 °C which falls within the specified limit of 3200 to 4800 Poise (IS 1206 1978). It is a common choice for the construction of major roadways such as national highways and expressways in India expecting a load repetition of more than 30 million standard axle (Mittal et al. 2018). It is highlighted that the VG-40 binder is particularly effective in areas where the traffic load and maximum pavement temperature is high. The use of VG-40 binder is recommended when maximum pavement temperature falls between 58 and 76 °C and traffic load is ≥ 20 msa (millions of standard axle). The use of VG-40 binder can be further extended subjected to a maximum of 50 msa traffic load with revised maximum pavement temperature of 64 °C (MoRTH 2013). The binder properties were assessed before using it in the sample preparation as shown in Table 1. As per Indian specifications (IS 73 2013), binders are classified based on viscosity, and there are no specific test protocols or specifications for performance grading and continuous grade at higher temperatures (Singh, Gupta, and Miljković 2023). Therefore, ASTM guidelines (ASTM D 6373 XXXX) were followed to evaluate the rheological characteristics using a dynamic shear rheometer.

3.2. Physical properties of aggregates

In this research, Granite (a siliceous aggregate) was used for the preparation of bituminous mix samples. Granite is frequently used in the preparation of flexible pavements in India. Prior to the preparation of the mix, the physical properties of the aggregates were examined, as shown in Table 2. As per the MoRTH (2013) guidelines combined flakiness and elongation index, abrasion

Table 1. Specification limit and physical properties of asphalt binder.

Properties	Values obtained	Test method	Specified limit	Status
Penetration value at 25 °C, 0.1 mm	41	IS 1203 (2022)	35 (min)	Accept
Absolute viscosity at 60 °C, Poises	4480	IS 1206-Part 2 (1978)	3200–4800	Accept
Softening point, °C	54	IS 1205 (1978)	50 (min)	Accept
High-temperature continuous grade, °C	77.2	ASTM D 6373 (XXXX)	Not available	Not available
High-temperature PG, °C	76	ASTM D 6373 (XXXX)	Not available	Not available

Table 2. Specification limits and physical properties of aggregates.

Properties	Combined flakiness and elongation index	Abrasion value	Impact value
Specification limit	Max 35%	Max 40%	Max 30%
Test protocol	IS:2386-Part I (IS 2386-1 1963)	IS:2386-Part IV (IS 2386-4,1963)	IS:2386-Part IV (IS 2386-4 1963)
Test results	19%	16.8%	14.6%
Status	Accept (within spec.)	Accept (within spec.)	Accept (within spec.)

value, and impact value test of aggregates has been conducted to check the suitability of its usages in various layers of the AC pavement.

3.3. Properties of asphalt concrete mix

Since, BC and SMA are common mixture types used in pavement construction, samples of BC-1, BC-2, SMA-1, and SMA-2 were prepared in the laboratory. Figures 1(a)–1(d) show the gradations of aggregates that were used for the preparation of the asphalt mixtures as per the per MoRTH (2013) guidelines. As can be seen from the figures, the target gradations selected for all the mixes fell within the maximum (upper bound) and minimum (lower bound) prescribed limits. Mixture samples were prepared following the Marshall mix design procedure (Singh, Gupta, and Miljković 2023) as recommended by the Indian specification (IRC 111 2009). The optimum binder content and other volumetric properties are given in Table 3. Similar to the practice adopted in field, SMA mixes were stabilized with 0.3% of pelletized cellulose fibers by weight of the total mix. As given in Table 1, the obtained values of binder properties were found within the specified limits of MoRTH (2013).

The OBC of SMA-1 was found highest among all four mixes considered in this study as it is a gap graded mixture with stone-to-stone contact of coarser aggregates and relatively lesser fine contents (20%–30% passing 2.36 mm IS sieve). The high binder content mastics composed of fine aggregates, fillers, asphalt binder, and stabilizing additives fills the voids and provides durability to the mix.

As shown in Fig. 1, SMA-1 and SMA-2 are relatively gap graded mixture as after 4.75 mm, only 9.5- and 13.2-mm particles are available in the aggregate gradation. Also, few sizes finer than 2.36 mm are missing in SMA gradations. However, BC are considered as dense graded mixture as almost every size of aggregate is present.

3.4. Properties of emulsion and stabilized aggregates

ETA is a cold mix base layer stabilization technique in which recycled aggregates or virgin aggregates are treated with slow-setting (SS) asphalt emulsion (Pérez, Medina, and del Val 2013; Chehelgo, Abiero Gariy, and Muse Shitote 2018; Andrews, Radhakrishnan, Koshy, Chowdary, et al. 2023). These emulsions are normally prepared by mixing water (25–60%), bitumen (40–75%), and emulsifier (0.1–2.5%) (Baghini et al. 2017). ETA is gaining popularity in India as it significantly improves cohesion and moisture resistance (Southern African Bitumen Association

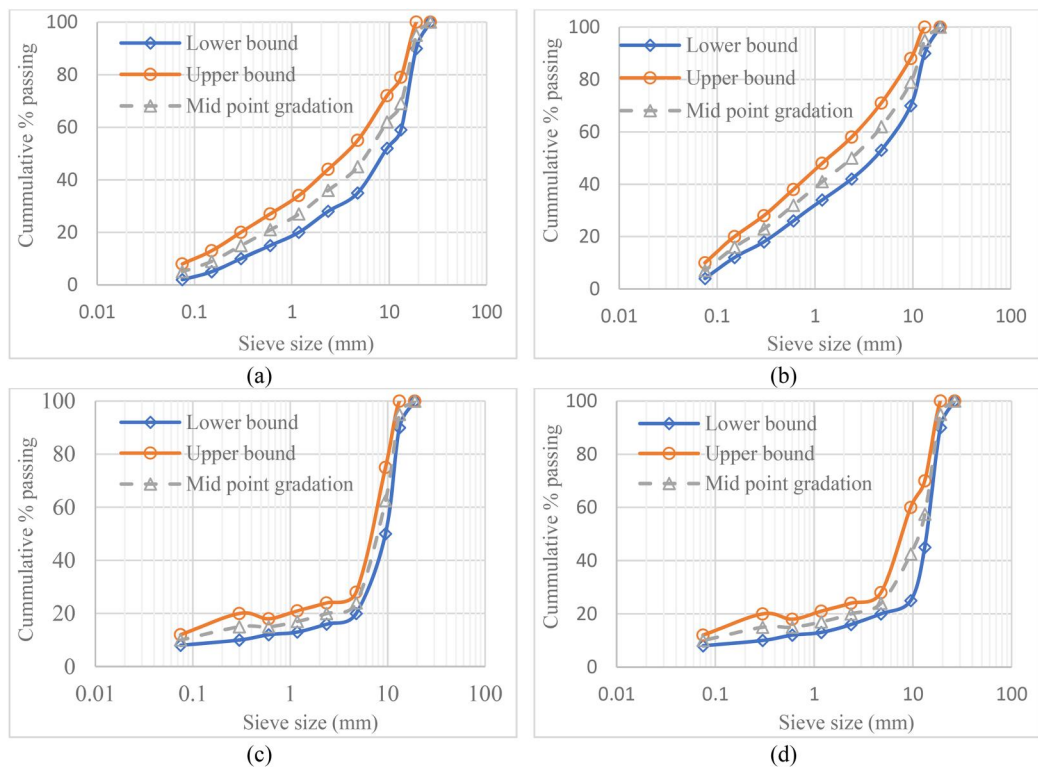


Figure 1. Specification limits and target (a) gradation of BC-1, (b) gradation of BC-2, (c) gradation of SMA-1, and (d) gradation of SMA-2.

Table 3. Volumetric properties of various mixes obtained from Marshall mix samples.

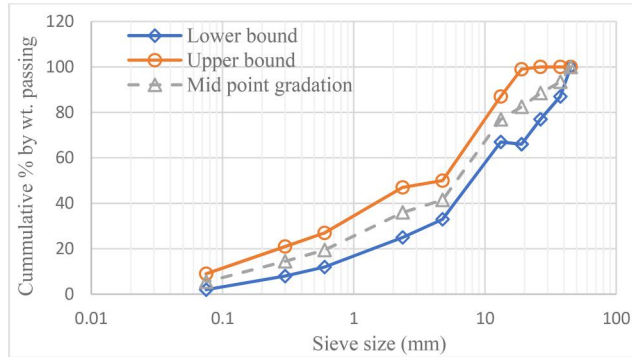
Mix type	Binder	OBC (%)	G_{mb}	G_{mm}	Air void (%)	VMA (%)	VFB (%)	Stability (kN)	Flow (mm)
BC-1	VG 40	5.52	2.376	2.374	4.271	13.123	67.457	15.684	3.240
BC-2	VG 40	5.70	2.414	2.470	3.887	13.195	70.546	14.216	3.196
SMA-1	VG 40	6.24	2.358	2.458	4.055	19.342	79.034	09.687	3.864
SMA-2	VG 40	5.52	2.376	2.374	4.271	13.123	67.457	15.684	3.240

(Sabita) 2002) due to the presence of thin bituminous film around the aggregates (Southern African Bitumen Association (Sabita) 2002). Since, granite aggregates are suitable for cationic asphalt emulsion, thus, SS-2 which is specially designed water-based bitumen emulsion with low viscosity and extended setting time was used in this study. Table 4 summarizes the properties and specification limits for SS-2 bitumen emulsion as per the guidelines of IS 8887 (2004).

Slow setting bitumen emulsion of cationic nature are generally used with the aggregates having high surface area to provide better coating and curing characteristics. The gradation of the aggregate used in this research is shown in Fig. 2, whereas, other technical details of ETA are shown in Table 5. In this research, the optimum fluid content (OFC) required for preparing the ETA mix was estimated as per the IRC guidelines (IRC 37-2012 2012). The SS-2 emulsion type, 4% by weight of the mix and 1% cement as the active filler was used to stabilize the aggregate base layer. The M_r value of ETA was obtained using the IT pulse modulus test (ASTM D 4123 1995).

Table 4. Properties of SS-2 bitumen emulsion.

Properties	Specification limits	Values obtained
Residue on 600 micron IS sieve	Max 0.05%	0.02%
Viscosity at 25 °C (Saybolt viscometer)	30–150 s	42 s
Storage stability after 24 h	Less than 2%	0.6%
Particle charge	Positive	Positive
Residue by evaporation	Minimum 60%	68%
Penetration at 25 °C/100 gm/5 sec	60–120 (1/10th of mm)	95
Ductility at 27 °C	Minimum 50 cm	>50 cm
Solubility in trichloroethylene	Minimum 98%	>98%

**Figure 2.** Aggregate gradation adopted for emulsion-treated aggregate stabilization.**Table 5.** Emulsion-treated aggregate mix properties.

ETA properties	Obtained values	Test protocol
Optimum fluid content	6.4%	IRC 37-2012 (2012)
Maximum dry density	2.12 g/cc	
Emulsion type	SS-2	Not available
Emulsion dosage	4%	IRC 37-2012 (2012)
Cement content	1%	
ITS (14 days)	232 kPa	ASTM D 6931 (2017a)
Resilient modulus at 35 °C	860 MPa	ASTM D 4123 (1995)

As shown in Fig. 2, the fine aggregates (<2.36 mm) in ETA constitutes 36% of the total weight which is significantly higher than in case of SMA-1 and SMA-2 (only 20%). However, BC mixes, specifically BC-2 has higher fine aggregate content (50%) than other asphalt mixes and ETA.

The selection of test temperature of 35 °C for resilient modulus test is based on the average annual pavement temperature in India as specified by the IRC (IRC 36-2018 2018). The temperature variation across the depth has not been considered in this study.

3.5. Moduli tests of asphalt mixtures

In this research, stiffness of asphalt mix samples was measured using M_r tests based on ITS peak load value using Dynamic Testing System (Karami et al. 2018; Usman and Masirin 2019; Singh and Gupta 2024). M_r was used in this research because it is a widely accepted method for characterizing bituminous mixtures (ASTM D 7369 2011). The M_r test was preferred because several measurements can be taken on the same specimen (Munoz et al. 2015) reducing the specimen-to-specimen variability. The samples were prepared with air voids of $7 \pm 0.5\%$. The required voids were achieved by reducing the number of blows from 75. The samples were

Table 6. Resilient modulus (MPa) of AC mixes at different test temperatures.

Mix type	Mix temperature (°C)		
	25	35	45
BC-1	2992	1826	618
BC-2	3373	2241	709
SMA-1	3134	1449	852
SMA-2	2809	1065	702

conditioned at test temperature for 4 h prior to testing. The conditioning period was 100 cycles and the M_r was calculated as average of the last five cycles of sequence 1 loading. The tests were repeated at three different temperatures of 25, 35, and 45 °C. A 10% of peak load (failure load) obtained from the ITS test (ASTM D 6931 2017b; Kumar et al. 2024) was used for M_r tests. The results of M_r values obtained for various asphalt mixes at different test temperatures are shown in Table 6.

The resilient modulus of SMA mixes, specially SMA-2 was found lesser at lower temperatures as compared to BC mixes; however, these are stiffer mixes at relatively higher temperature. Elastic recovery in SMA mixes in M_r test was found significantly lower than BC mixes at higher temperatures.

3.6. Material characterization of unbound granular layers

Aggregates and soil, treated as unbound granular materials (UGMs) are used in the base, subbase, and subgrade layers of the asphalt pavement, serving a crucial role in load distribution. The shear resistance of aggregate skeleton through interlocking of particles gives the bearing capacity to UGMs. UGM's response to cyclic loading is not purely elastic, and some plastic deformation occurs in each cycle. The strain induced in each cycle comprises an elastic strain and a plastic strain. The elastic part of the strain is recoverable on unloading, while the plastic part is permanent. These materials under repeated load, exhibit nonlinear stress-dependent behavior. Stress-dependent behavior of materials used in unbound granular layers is generally evaluated using the repeated load triaxial compression testing. It requires advanced test apparatus like Dynamic testing system (DTS) or Universal testing machine (UTM) to conduct repeated load triaxial testing which is not readily available in many research laboratories in growing economies like India (Singh, Behl, and Dhamaniya 2022). In absence of it, material characterization of base, subbase, and subgrade layers has been primarily based on the CBR values of the supporting soil layer. Hence, material properties of these layers were evaluated using M_r values. The Indian design code IRC (IRC 36-2018 2018), prescribes empirical relations (Eqs. (1)–(3)) for calculating the M_r values of various unbound layers.

$$M_{rs} = 10 \times CBR \text{ for } CBR \leq 5\% \quad (1)$$

$$M_{rs} = 17.6 \times (CBR)^{0.64} \text{ for } CBR > 5\% \quad (2)$$

where M_{rs} is resilient modulus of the soil in subgrade layer (MPa). As recommended by IRC (IRC 36-2018 2018), the unbound aggregate layers were treated as a single layer, hence, a combined modulus value was attributed. The M_r of this granular layer was then calculated based on the combined thickness and the modulus of the subgrade layer.

$$M_{r(\text{granular})} = 0.2 \times (h)^{0.45} \times M_{rs} \quad (3)$$

where $M_{r(\text{granular})}$ is the combined resilient modulus of the base and subbase layer, measured in MPa, h is combined thickness of these layers, and M_{rs} is resilient modulus of the subgrade layer.

Table 7. Material properties of subgrade, subbase, and base layers.

S no.	Pavement layers	Thickness (mm)	CBR (%)	M_r (MPa)	ν
1	Subgrade layer	500	10.80	80	0.35
2	Subbase layer	350	N.A.	295	0.35
3	Base layer	300	N.A.	295	0.35

Note: N.A.: not applicable

Material properties of the subgrade, base, and subbase layers used in this study are presented in Table 7.

4. FE modeling of tire-pavement system

Performing research studies in field is generally labor intensive, time-consuming, and expensive. Due to advancements in computational facilities in modern days, properly calibrated FEM tools have proven to be a good alternative (Kumar et al. 2023). In this research, to simulate the effect of base stabilization *via* ETA, loading conditions, mix behavior, and layer thickness on pavement response, a three-dimensional FE model of tire-pavement system using solid tire and deformable AC pavement was developed in this study. The tire was modeled to consider nonuniform contact stress distribution at the tire-pavement interface. The layer interaction properties (friction formulation) can also be defined in the FE simulation. These complexities (nonuniform loading and layer interactions) cannot be handled using analytical solutions of asphalt pavement. The following subsections present a brief description of the FE modeling technique.

4.1. FE modeling of pavement layers

In the developed FE model, all the pavement layers were assumed to be linear elastic material. The advantages of using linear materials are two-fold. Linear elastic assumption significantly reduces the total computation time. Moreover, the current design practices in many developing nations are based on linear elastic theories, hence the interpretation of data will be easier for practitioners and researchers. A conventional asphalt pavement system with four layers, AC (wearing and binder course), granular base, subbase, and compacted subgrade layer over natural formation was modeled. In this study, Penalty friction formulation has been considered to define the interaction between layers. It makes the simulation more realistic. The friction coefficient at the interface of the various layers has been determined using Newton's inclined plane test. In this test, sample specimen of unbound granular layers is compacted at maximum dry density and optimum moisture content while asphalt samples are compacted at design air void. In this test, the two samples between which friction coefficient need to be calculated is marked as lower and upper layer samples. For example, in the computation of friction coefficient between subgrade and subbase layer samples, subgrade samples will be marked as lower surface whereas subbase sample will be marked as upper layer. The lower layer sample as they are laid in the field is glued to a fixed platform and the upper layer sample is kept over it to move freely. The inclination of the platform is kept on increasing slowly till the moment where upper layer sample starts slipping over the lower layer sample. This inclination is noted and tangent of it is recorded as friction coefficient at the interface of the two layers. This method has certain limitations as slipping of one layer over the other starts in field under the cyclic loading which has not been simulated in this test. This test may produce friction coefficient values on the conservative side in absence of loading. The other limitation is the lower layer is fixed with the platform which is not allowed to slide over it, however, in field, no layer is completely fixed. So, relative movement of the fixed layer in contact has been ignored. However, this test is easy, convenient, and fast to provides a fair idea of friction between the two surfaces in contact. The details of measured friction

Table 8. Layer interaction properties (friction coefficient) at the interface.

S No.	Surface in contact	Sliding angle	Friction coefficient
1	Asphalt concrete – conventional base (WBM)	33.82°	0.67
2	Asphalt concrete – stabilized base (ETA)	31.38°	0.61
3	Conventional base (WBM) – subbase	35.75°	0.72
4	Stabilized base (ETA) – subbase	32.21°	0.63
5	Subbase – subgrade	27.47°	0.52

coefficient at the interface of various layers have been shown in Table 8. The friction coefficient at the interface of base (WBM/ETA) and asphalt layer has been obtained after the application of SS-1 emulsion as prime coat at the rate of 10 kg/10 m² area over the base layer. The application of prime coat is based on the guidelines of IRC: SP 100 (use of cold mix technology in construction and maintenance of roads using bitumen emulsion).

The roughness of granular subbase layer was found highest among all the given layers hence a higher friction coefficient at conventional base-subbase interface was found compared to other interfaces. The simulation of layer interaction properties makes FE based analysis more realistic which is not possible in analytical methods.

4.2. FE modeling of test tire

The current design method of AC pavement assumes a circular contact area and uniform distribution of vehicle load, which could significantly differ from the actual field conditions (Dwyer-Joyce and Drinkwater 2003; Jiang et al. 2019). The assumption is used because it simplifies the calculation in pavement analysis. However, it is difficult to explain the behavior of distresses in AC pavement gradually developing from the surface under heavy vehicles using a simple uniform loading in FE analysis (De Beer, Fisher, and Jooste 2002; Siddharthan et al. 2002; Jiang et al. 2019; Oubahdou et al. 2021). Therefore, it is necessary to consider nonuniform contact stress distribution in the FE model (Wang and Al-Qadi 2010). A three-dimensional test tire was modeled to simulate the complex stress distribution over the loading area. Solid tire in India is generally used in forklift trucks and construction equipment. Solid tires are more popular in heavy-duty vehicles due to their ability to withstand excessive loads and operational capability in harsh environments (Phromjan and Suvanjumrat 2018). It is also easy to evaluate the material properties of solid tire as it consists of single rubber material. For modeling tire rubber, the suitable hyper-elastic material model was obtained using relevant tensile test data and a curve fitting approach (Premarathna et al. 2020). Hyper-elastic models are generally used to calculate elastomer's properties that respond elastically when subjected to large deformations (Li, Liu, and Frimpong 2012). These material models are expressed in the form of polynomial functions. The generalized strain energy density function for incompressible materials is explained as shown in Eq. (4).

$$U = U(F) - P(J - 1) \quad (4)$$

where J is determinant of the deformation gradient matrix and U(F) can be expressed as shown in Eq. (5):

$$U(F) = U(I_1, I_2, I_3) = U(\lambda_1, \lambda_2, \lambda_3) \quad (5)$$

where I_1, I_2 , and I_3 are the first, second, and third strain invariant and λ_1, λ_2 , and λ_3 are the primary elongation (Hossain and Steinmann 2013). The Yeoh hyper-elastic material model was selected using the curve fitting method to describe the mechanical behavior of test tire rubber. The constitutive Yeoh model for compressible rubber is presented in Eq. (6).

Table 9. Coefficients of material model for solid tire.

Material	Coefficient (MPa)		
Rubber	C_{10}	C_{20}	C_{30}
	0.684	-0.022	0.007

$$W = \sum_{i=0}^3 C_{10} (\bar{I}_1 - 3)^i \quad (6)$$

where W is the strain energy density function, \bar{I}_1 is the first principal invariant and C_{10} is the material constant. The material constant C_{10} is interpreted as half the initial shear modulus. Table 9 shows the material model constants used in the analysis.

4.3. FE modeling of tire-pavement interaction

In this research, the developed model uses contact approaches as proposed by previous researchers (Anupam et al. 2021; Premarathna et al. 2021). As a first step, the contact between the two interacting surfaces of tire-pavement bodies is defined (Shoop 2001). Both the surfaces (tire and pavement) are considered as deformable, the tire being considered a slave surface whereas the pavement surface was considered a master surface. A finer mesh in the tire region was considered as nodes on the slave surface were not allowed to penetrate the master surface. The interfacial contact was defined using the Penalty function (see Eq. (7)) and a tangential contact was defined using the Coulomb friction model as shown in Eq. (8). More details about the contact formulation can be found elsewhere (Wang, Al-Qadi, and Stanciulescu 2012).

$$F_n = \begin{cases} S_n C & C \leq 0 \\ 0 & C > 0 \end{cases} \quad (7)$$

$$F_t = S_t \delta^e \quad (8)$$

where F_n is the normal interaction force, F_t is tangential interaction force, S_n and S_t are normal and tangential contact stiffness respectively, C is the clearance value of the node in contact relative to the target surface, and δ^e represents elastic deformation of the contact node relative to the target surface.

4.4. Description of element type and boundary conditions

Pavement depth is considered to be 6 m in vertical direction (-z) to represent the semi-infinite layer below the compacted subgrade as shown in Fig. 3. The eight-node hexahedral brick element was considered to model pavement layers. A higher number of elements (fine meshing) closer to the loading area and a lesser number of elements (relatively coarser mesh) away from the loading area were considered as shown in Fig. 3. The friction coefficient between pavement surface and tire is kept 0.35 as considered in past studies (Gupta et al. 2021). The element size in AC layer closer to loading area is kept 30 mm × 30 mm while it is 70 mm × 100 mm away from the loading area. In lower layers of the pavement, element size is kept 30 mm × 100 mm closer to loading area while 70 mm × 100 mm away from the loading area. The element size of the outer surface of solid tire is kept 15 mm × 15 mm in this study.

To simulate realistic field constraints, elements in the longitudinal direction (4 m) of AC pavement were kept free to move. The elements in the transverse direction (2 m) were constrained (fixed boundary) as it is supported by the shoulder area. Movement of all the nodes in the

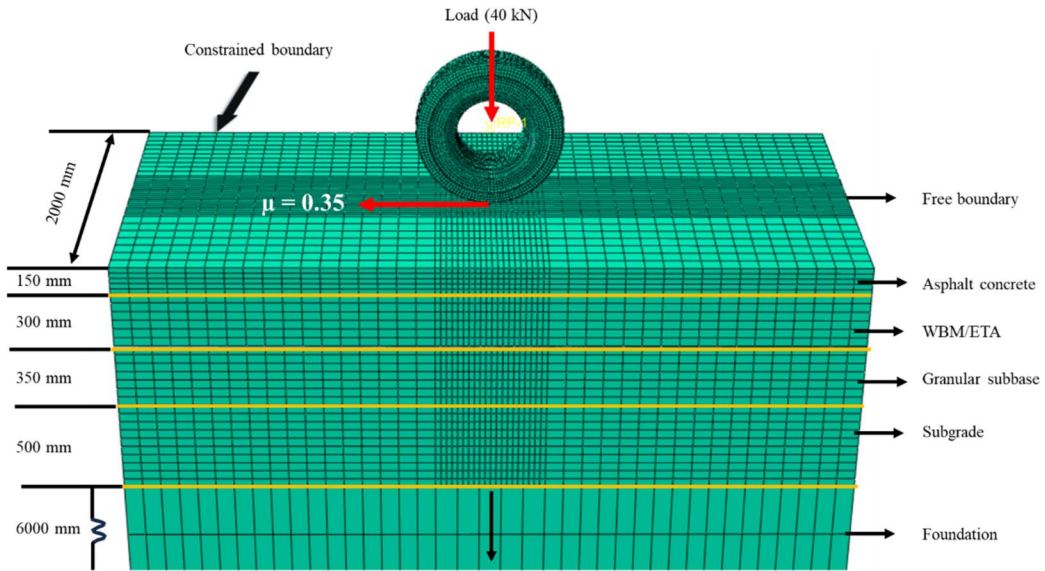


Figure 3. Solid tire loading and meshing.

vertically downward direction was allowed. The bottom elements of natural foundation were fixed in all degrees of freedom as stress to this depth generally subsides to zero.

4.5. Validation of the model

To check the accuracy of the model, the FE model of tire-pavement system was validated using responses obtained from 3D Move Analysis (Nasimifar, Thyagarajan, and Sivanewaran 2017) software. The contact area corresponding to different tire loads and maximum vertical deformations in the AC layer were selected as response criteria. The FE simulations were carried out considering BC-2 mix ($E = 3000$ MPa and $\nu = 0.35$) with a conventional base (WBM) layer with the identical input parameters of 3D Move Analysis (Nasimifar, Thyagarajan, and Sivanewaran 2017). The considered material properties of unbound granular layers were obtained from laboratory testing as shown in Table 7. Figure 4 shows a comparison of the predicted contact area and maximum AC deformations under different loading levels.

As shown in Fig. 4, a good agreement was found between the results obtained from 3D Move Analysis and the proposed FE model. A maximum difference of 5.87% in the estimated contact area from the two methods as shown in Fig. 4(a) was found. As shown in Fig. 4(b), a maximum difference of 5.37% in maximum vertical deformation was found. The average difference in contact area was found to be 3.39% while 2.61% for maximum deformation. Considering the apparent difference between FE and 3D Move software, the difference can be taken as relatively small.

5. Results and discussion

The pavement performance during its intended design life depends on a number of factors like materials used in various layers, loading conditions, and environmental conditions. The use of suitable materials especially in the AC layer is important as highest portion of the stress is absorbed in this layer itself. Other than the mixture properties, temperature and

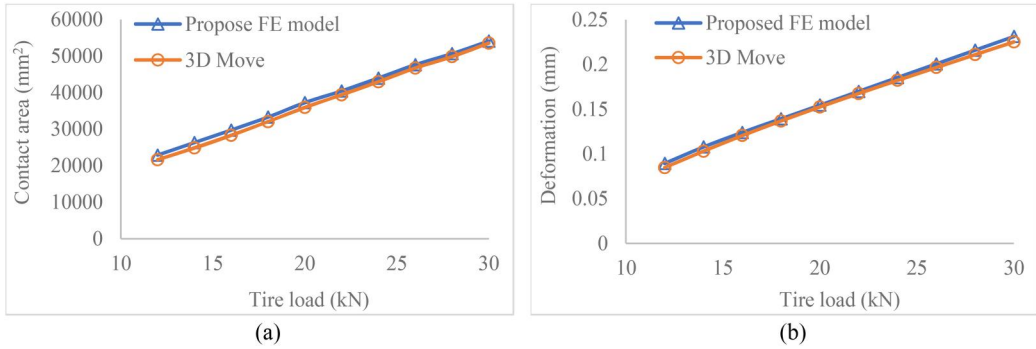


Figure 4. Variation of (a) contact area and (b) maximum deformation in AC layer with different tire loads.

loading conditions are other important factors for the pavement design. Hence, in the first stage of the simulation, the validated FE model (see Section 4.5) was utilized to study a standard pavement cross-section. The effect of different tire loads (including over-loading), mixture type, temperature, and layer thicknesses on the structural response was analyzed. The data obtained from these simulations were used for the relative comparisons. In the second stage of the simulation, the base layer was replaced with the ETA layer to study the effect of emulsion-treated base on pavement responses. The goal of the second stage of the simulation was to check if the ETA stabilization technique can help in the reduction of top-layer and conventional base thickness without compromising pavement performance. Since, rutting and fatigue is a common distress type, the performance of the pavement was evaluated considering these two. Subgrade rutting and AC fatigue life were calculated on the basis of empirical relations (Eqs. (9)–(11)).

These relations (Eqs. (9)–(11)) are calibrated for evaluating design life considering unbound granular layers. The design code in India (IRC:37) also provides separate models for fatigue damage analysis in cement treated base (CTB). However, there is no separate guidelines (performance model) available for finding design life of asphalt pavement in case of emulsion stabilized base. The transfer function used for the evaluation of asphalt fatigue life is valid and can be used in emulsion stabilized base also as no practical variations are observed with the change in lower layer stiffnesses. In practice, these transfer equations as stated above are being used with emulsion stabilized base also. However, extensive field and laboratory test data is required to develop a reliable model in this case.

The models given by Eqs. (9)–(11) has been prescribed for 90% reliability in IRC (IRC 36-2018 2018). The reliability is considered as the probability that pavement will actually perform at or above the estimated performance level. These guidelines recommend 90% reliability performance equations for all important roads like expressways, national highways, state highways, and urban roads. For other categories of roads, 90% reliability equations are used for design traffic of 20 msa or more. For design traffic of less than 20 msa, 80% reliability performance models can be used as specified in IRC (IRC 36-2018 2018). The outcome of the simulations could be of particular interest to the policy makers as currently no design guidelines are available. For ease of understanding, the results are summarized in the following subsections.

$$N_R = 1.41 \times 10^{-8} \left(\frac{1}{\varepsilon_z} \right)^{4.5337} \quad (9)$$

where N_R is rutting life of subgrade (measured as cumulative equivalent number of 80 kN standard axle load served by pavement before the rut depth of 20 mm or more) and ε_z is the vertical compressive strain at the top of the subgrade layer.

$$N_f = 0.5161 \times C \times 10^{-4} \left(\frac{1}{\epsilon_t} \right)^{3.89} \times \left(\frac{1}{M_r} \right)^{0.854} \quad (10)$$

$$C = 10^M \text{ and } M = 4.84 \left(\frac{V_{be}}{V_a + V_{be}} - 0.69 \right) \quad (11)$$

where N_f is fatigue life of asphalt layer (cumulative equivalent number of 80 kN standard axle load served by pavement before the critical cracked are of 20% or more), V_{be} is percent volume of effective binder in the mix, V_a is air void in the mix (%), ϵ_t is the horizontal tensile strain at the bottom of AC layer, and M_r is the resilient modulus of the AC mix. N_R and N_f have been evaluated in millions of standard axle (msa) load repetitions.

5.1. Structural response of asphalt pavement considering conventional base layer

This section discusses effect of critical parameters like loading, types of asphalt mixes, thicknesses of various layers, and environmental conditions like temperature on the structural response of asphalt pavement considering conventional base layer (WBM). These parameters (load, material properties, and temperature) have significant role in pavement damage and have been intentionally considered in this analysis. In later section, role of emulsion stabilized base will be analyzed, these results can be used as reference to understand potential benefits of stabilization.

5.1.1. Effect of loading

In line with the research scope, the effect of heavy vehicles (single, tandem, and tridem axle) on the structural response of the pavement was studied using conventional WBM as base layer. The maximum permissible axle weight in India for single, tandem, and tridem axle varies from 3 to 9 tonnes i.e., per axle (30 kN to 90 kN). However, the standard axle load considered for pavement analyses as per IRC (IRC 36-2018 2018) recommendations is 80 kN. For simplicity, the load can be considered as evenly distributed, hence, half of the loads (40 kN) were considered as single-tire load. Input parameters of the FE model (see Fig. 3) such as M_r and ν of the unbound layers are given in Table 7, while material properties of BC-2 used as top layer in the pavement is provided in Table 6. The Poisson's ratio is considered as 0.35 for BC-2 as specified by IRC (IRC 36-2018 2018). The effect of an increase in tire loading on pavement responses, vertical deformation, ϵ_z , ϵ_t , σ_z , and σ_t are shown in Figs. 5(a)–6(d) respectively. The vertical compressive stress (σ_z) and tensile stress (σ_t) were evaluated at $z=150$ mm. To make ease of understanding, the data of Fig. 5 is presented in tabular form with their respective % changes in Table 10. All the changes in deformations, ϵ_z , and ϵ_t values at various load levels as shown in Table 10 is with respect to 20 kN load.

As shown in Fig. 5(a), the vertical deformation decreases with an increase in the pavement depth and increases with an increase in the tire load. Maximum vertical deformation is observed at the pavement surface (directly below the tire load) as stress is highest at this point and gradually decreases with the pavement depth as stress disperses to larger area. An increase in vertical load from 20 kN to 25 kN results in an increase of 21.87% in vertical deformation in the AC layer (see Table 10). It is further observed that the effect of the increasing load is more significant in the upper layers of the pavement as the load is directly coming over the top surface and reduces significantly after the AC layer.

As shown in Fig. 5(b), the variation of vertical compressive strain, ϵ_z with depth was found to vary non-linearly. Initially, the strain ϵ_z was found to increase with depth until a critical point is reached. After the critical location ($z=200$ mm), a sharp decrease is observed till the subbase-subgrade interface ($z=800$ mm). The observed behavior is similar to the findings of past research

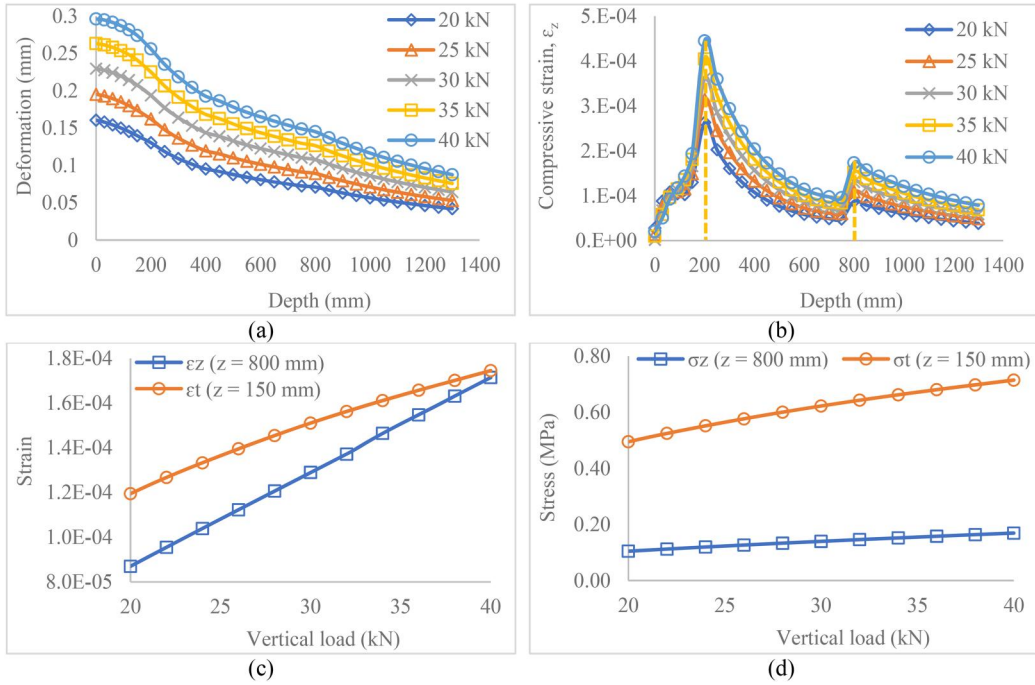


Figure 5. Effect of single tire load on (a) deformation, (b) compressive strain, (c) ϵ_z and ϵ_t and (d) σ_z and σ_t .

studies (Pan et al. 2021; Yao et al. 2021). The slope change at the interface may be due to a significant reduction in stress at that point.

As shown in Fig. 5(c), it was found that an increase in vertical load affects ϵ_z more prominently than ϵ_t . It was found that for an increase of 5 kN load from 20 kN to 25 kN, ϵ_z increases by 24.25% while ϵ_t increases by 14.23% for the same increment in load (see Table 10). Similarly, as shown in Fig. 5(d), the values of σ_z and σ_t at a depth of 150 mm were evaluated. An increase of 61.75% in σ_z was observed for a change in load from 20 kN to 40 kN, however, σ_t was found to increase by 44.37% for the same change in vertical loading. Table 10 also shows that an increase in load significantly reduces the rutting and fatigue life of the pavement. For example, an increase of 5 kN load from 20 kN to 25 kN, reduces the rutting life of the subgrade layer by 62.63% and fatigue life of the AC layer by 40.67%. From the above observations, it can be clearly seen that the developed FE model can appropriately capture the pavement response behavior.

5.1.2. Effect of mix type and temperature

In line with the objective of the study, the effect of temperature on pavement responses at different temperatures was studied considering conventional base layer. The composition of pavement and material properties are same as considered in Section 5.1.1. In India, the average annual temperature falls near 25°C and reaches to 45°C in summer, so a temperature range 25°C–45°C was considered. Effect of temperature on M_r values of AC mixes was evaluated and same has been considered to analyze its effect on structural response of the pavement. Pavement responses in terms of vertical deformation and ϵ_z were studied for all the mixtures, as shown in Figs. 6(a)–6(h).

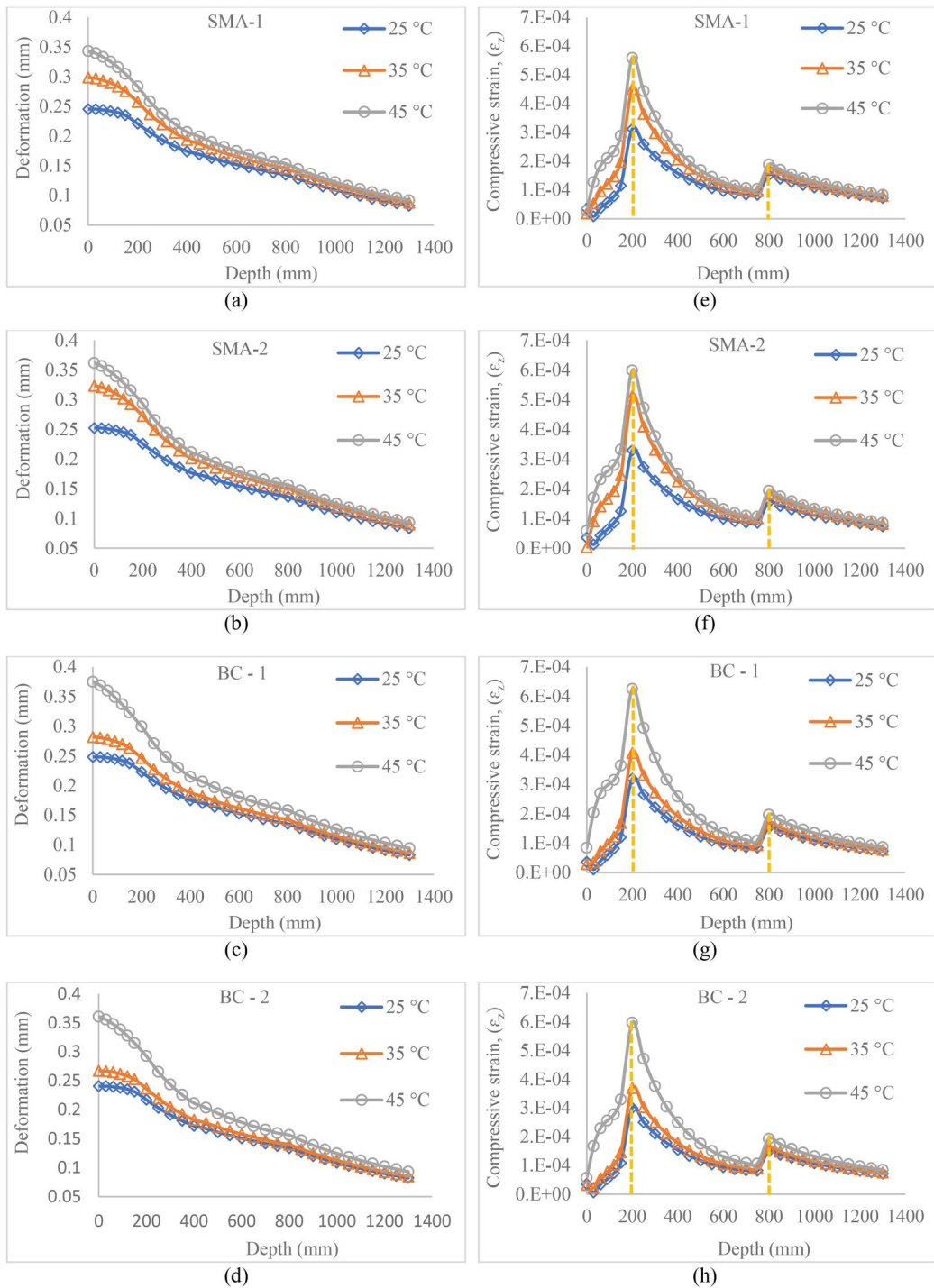


Figure 6. Effect of temperature on pavement deformation and normal compressive strain at 40 kN load.

Table 10. Variation of maximum deformation, strains, and pavement life with vertical load.

Load	20 kN	25 kN	30 kN	35 kN	40 kN
Maximum deformation (mm) in AC	0.160	0.195	0.229	0.263	0.296
% increase in deformation	–	21.87	43.12	64.37	85.00
ϵ_z (micro-strains) at top of the subgrade	87.0	108.1	129.0	150.6	171.5
% increase in ϵ_z		24.25	48.27	73.10	97.12
ϵ_t (micro-strains) at bottom of the AC	119.5	136.5	151.1	163.5	174.6
% increase in ϵ_t	–	14.23	26.44	36.82	46.10
Subgrade rutting life, msa (N_R)	36,159	13,510	6062	3004	1667
Fatigue life of AC layer, msa (N_f)	236	140	94	69	54

Table 11. Effect of AC mixes and temperature on the structural response of pavement.

AC mix	Temp (°C)	Max. deformation in AC layer (mm)	% increase	ϵ_z (z = 800 mm) (microstrains)	% increase	Subgrade rutting life, msa (N_R)
SMA - 1	25	0.245	N.A.	152.2	N.A.	2864
	35	0.298	21.63	174.2	14.45	1553
	45	0.343	15.10	188.2	08.04	1094
SMA - 2	25	0.252	N.A.	155.5	N.A.	2599
	35	0.323	28.17	182.4	17.30	1261
	45	0.362	12.07	193.2	05.92	971
BC - 1	25	0.248	N.A.	153.6	N.A.	2748
	35	0.281	13.30	167.9	09.31	1835
	45	0.375	33.45	196.5	17.03	900
BC - 2	25	0.241	N.A.	149.9	N.A.	3069
	35	0.267	10.79	162.1	8.14	2152
	45	0.361	35.20	193.0	19.06	976

Note: N.A.: not applicable.

As expected, figures (Figs. 6a–6d) show that pavements prepared with different mixes result in significantly different responses under same loading conditions. While assessing the role of temperature, it can be seen that the higher the surrounding temperature, the higher the pavements become sensitive to the type of mixtures. This could be explained by the fact that at lower temperatures, all the mixes are stiffer to the same limit. On the basis of data obtained from Fig. 6, Table 11 was prepared to compare the relative performances of the mixture.

As shown in Table 11, at higher temperatures, the percentage change in vertical deformation in the AC layer and ϵ_z is found to be higher for BC samples than the SMA samples which implies that the effect of temperature was also found to be more prominent on BC mixes as compared to SMA mixes. For example, maximum deformation in the AC layer was found to increase by 33.45% and 35.20% for BC-1 and BC-2 mixes respectively when temperature increases from 35 to 45 °C. However, for the same change in temperature, the increase for SMA-1 and SMA-2 mixes are found to be 15.10% and 12.07%, respectively. This could be explained by the fact that at lower temperatures, binder is stiff in the mix and BC offers more resistance to applied load due to relatively denser gradation. However, at the higher temperature, viscosity of binder reduces significantly, and load is mainly resisted by the aggregate skeleton. Since, SMA mixes are composed of a higher fraction of coarser particles, aggregate-to-aggregate contact is more effective. These findings support the usage of SMA mixes at extreme pavement temperatures where relatively higher deformations are expected. To understand the effect of temperature on the rut response of the AC mix, material properties (M_r) at extreme pavement temperatures were evaluated, which will be discussed in the following paragraph.

The asphalt mix stiffness is quite sensitive to temperature. An increase in temperature reduces resilient modulus of the mix. In the current design guidelines, it is recommended that grades suitable for temperatures nearest to the specified maximum should be adopted (IRC 36-2018 2018). The maximum pavement temperature is important for understanding which grade of binder

Table 12. Maximum pavement temperature (IRC-SP-135 2022) and M_r of asphalt mix for different regions in India.

City	State	Air temp (°C)	Pavement temp (°C)	Region	M_r (MPa)	N_R (msa)	N_f (msa)
Delhi	Delhi	45	66.87	Northern	339	811	63
Srinagar	J&K	28	50.74		727	1167	46
Phalodi	Rajasthan	51	73.00		224	680	91
Surajpur	Chhattisgarh	46	68.30	Central	304	772	69
Munger	Bihar	47	69.11	Eastern	288	755	72
Jalpaiguri	West Bengal	34	56.60		582	1045	48
Guwahati	Assam	45	67.13		328	799	65
Mumbai	Maharashtra	35	57.93	Western	542	1011	49
Himmatnagar	Gujarat	42	64.46		388	863	57
Tirumangalam	Tamil Nadu	40	62.26	Southern	438	912	54
Udupi	Karnataka	37	59.68		495	966	51
Vizianagaram	A. P	48	70.34		264	727	78

would be suitable for designing asphalt mixes. The average of seven days maximum air temperature for the hottest month is recorded and used for the determination of the maximum pavement temperature at a depth of 20 mm from the surface as specified in IRC (IRC 36-2018 2018).

$$T_{20mm} = [(T_{air} - 0.00618 \times Lat^2 + 0.2289 \times Lat + 42.2) \times 0.9545] - 17.78 \quad (12)$$

where, T_{20mm} is pavement temperature at a depth of 20 mm from the surface, T_{air} is average of maximum temperatures (°C) of seven days, and Lat is latitude of the place. It should be noted that these temperature variations do not include potential climate change effect on maximum temperature and needs further study. The maximum pavement temperature prevailing in different parts of India together with suggested M_r values are shown in Table 12.

Though these temperatures do not last long, they may play a vital role in the selection of suitable binder and deciding mix performance during their lifetime. Figure 7 presents the effect of maximum pavement temperature as experienced for various cities in India on ϵ_z at the top of the subgrade layer, ϵ_t at the bottom of the AC layer, and maximum vertical deformation in the AC layer.

As shown in Fig. 7(a), ϵ_z and ϵ_t were not found to be sensitive to changes in maximum pavement temperature. Compressive strain (ϵ_z) at the top of the subgrade was found to increase only by 12.67% with a change in maximum pavement temperature of 50.74 °C (Srinagar) to 73 °C (Phalodi). Horizontal tensile strain (ϵ_t) at the bottom of AC layer was found to increase by 8.71% for the same change in temperature. For the same increase in the temperature, N_R was found to decrease by 41.78%, whereas, N_f was found to increase by 97.82%. One of the reasons for the trend is because of the significant increase in the vertical deformation of the AC layer (see Fig. 7b). These outcomes indicate that both the fatigue life of the AC layer and subgrade rutting are significantly affected by temperature variation, hence, proper attention should be given at the design phase to enhance their durability.

5.1.3. Effect of layer thickness

In order to study the effect of layer thickness variation on the selected pavement structure, sensitivity analyses of layer thicknesses with respect to their structural responses as shown in Figs. 8(a) and 8(b) were done using WBM as base layer. The subgrade rutting (N_R) and fatigue life of the AC layer (N_f) were also estimated (see Figs. 8c and 8d). In the FE model (see Fig. 3), AC layer thickness was varied in the range of 100 mm to 200 mm, whereas, base layer and subbase layer thickness were varied between 150 mm to 310 mm. These ranges were selected as per the minimum specified limit (IRC 36-2018 2018).

As shown in Fig. 8(a), a reduction of 32.64% in ϵ_z was found when AC thickness increased from 100 mm to 200 mm, whereas, a reduction of 22.17% and 23.25% was found when base and

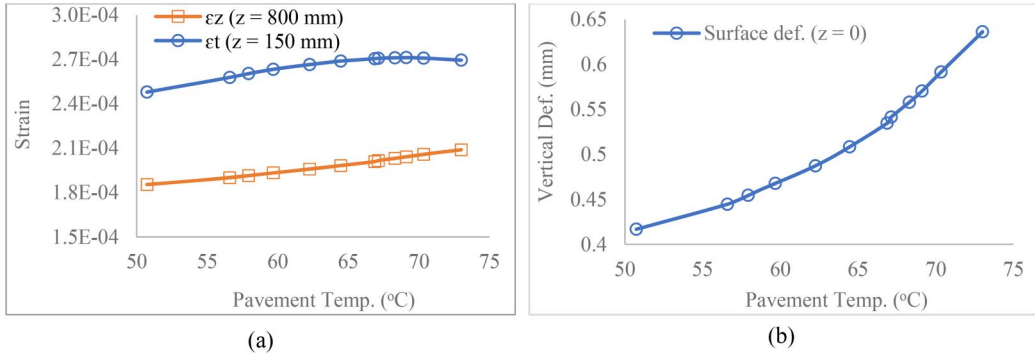


Figure 7. Effect of maximum pavement temperature on (a) strains and (b) vertical deformation of AC pavement.

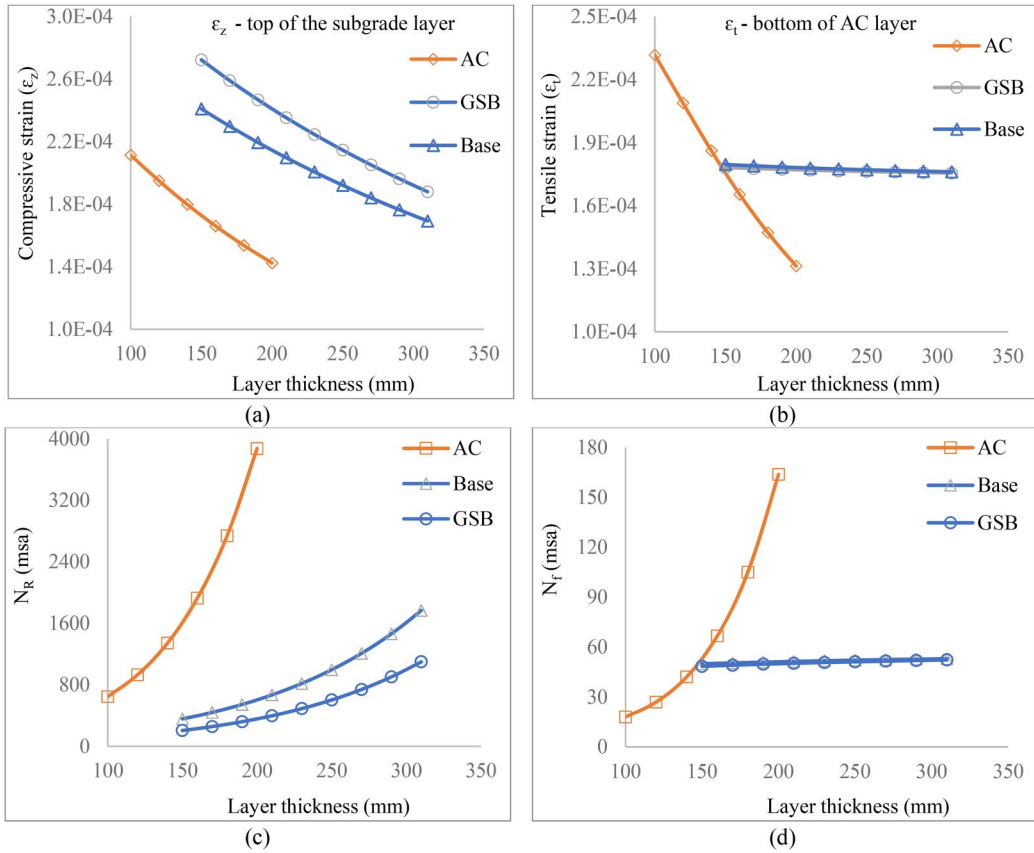


Figure 8. Effect of layer thickness on (a) ϵ_z , (b) ϵ_t , (c) N_R , and (d) N_F .

subbase layer thickness was increased in the same range respectively. Although an increase of thickness by 100 mm in the AC layer, reduces ϵ_t by 43.33% (see Fig. 8b), however, with the same increase in thickness in the base and subbase layer the values reduce by 1.07% and 1.40% respectively. On the basis of the obtained values ϵ_z and ϵ_t , pavement life against rutting and fatigue was

evaluated as shown in Figs. 8(c) and 8(d). It was found that, subgrade rutting life (N_R) improves by about 500% (see Fig. 8c) with an increase of 100 mm of AC thickness from 100 mm to 200 mm, whereas, an improvement of 179% and 194% was observed with the similar changes in base and subbase layer thickness. Similar plots for fatigue life (N_f) in Fig. 8(d), show that fatigue life performance improves by about 811% for the AC layer; however, no significant effects of 4.26% and 5.60% were observed in the base and subbase layer, respectively.

5.2. Structural response of asphalt pavement considering emulsion stabilized base layer

As discussed earlier in Section 3.4, ETA is becoming one of the popular choices in the pavement community due to its enhanced performance as a stabilized layer. It is apparent that the inclusion of the ETA layer will strengthen the whole pavement structure, however, the exact benefit in percentage is yet unknown, particularly in other higher layers. The FE model proposed in an earlier section (see Section 4), was used to have a deeper insight. This section discusses potential of emulsion stabilized base in reducing asphalt layer and conventional base layer thickness. The later subsection discusses overloading leverage in case of stabilized base layer as compared to conventional base pavement.

5.2.1. Potential of emulsion stabilized base in reducing asphalt and base layer thickness

At first, considering the same cross-section of pavement with the same loading the percentage enhancement in the performance was studied considering a layer with WBM (material properties as shown in Table 7) as a reference. After that, parametric analyses were carried out in which the AC layer thickness was reduced in sequence for both the reference structure (with WBM) and the structure with the ETA layer (material properties as shown in Table 5). The effect of ETA on maximum surface deformation ($z=0$) and strain (ϵ_t and ϵ_z) were analyzed as shown in Figs. 9(a) and 9(b) for comparison with a conventional base layer. The percentage change in critical strains ϵ_t and ϵ_z were evaluated for both the pavement structures (WBM and ETA) as shown in Figs. 9(c) and 9(d). These strain values were further used to estimate AC fatigue and subgrade rutting life as shown in Table 13. On the basis of the output of the analyses, a table (see Table 13) was presented which summarizes different combinations of thickness and the response of structure.

As shown in Fig. 9(a), it was found that the use of ETA results in a significant reduction in maximum deformation in the AC layer. For example, AC deformation in the case of 150 mm ETA base was found to reduce by 19.84% as compared to the same thickness of the conventional base. This reduction in AC deformation further increases with the increase in ETA thickness. The critical strains, ϵ_t and ϵ_z as shown in Fig. 9(b) were found to decrease with an increase in AC layer thickness for both conventional and ETA base pavement. The comparative changes in strain values for two different base layers were evaluated as shown in Figs. 9(c) and 9(d). It was observed that for a thinner AC layer (100 mm), the percentage change in ϵ_t (88.77%) and ϵ_z (28.13%) is more compared to thicker AC (200 mm) 59.56% and 21.62% respectively. Thus, it can be concluded the effect of ETA stabilization is more prominent for lower AC thickness. From the above analysis, it can also be seen that the effect of ETA on ϵ_t is much higher (maximum of 88.77%) than as compared to ϵ_z (maximum of 28.13%).

Parametric analysis with varying thicknesses of the AC layer was done. As shown in Table 13, for the same thickness of the conventional base as that of ETA (300 mm), the rutting life of the subgrade with ETA was found to improve by 142.90 to 207.62% when AC thickness varies from 200 to 100 mm. For similar conditions, the fatigue life of the AC layer was found to improve by 515.83 to 1006.25%. It can be concluded that, ETA has a higher impact on the fatigue life of the AC layer as compared to the rutting life of the subgrade and it improves fatigue performance of the pavement manifold as compared to rutting performance.

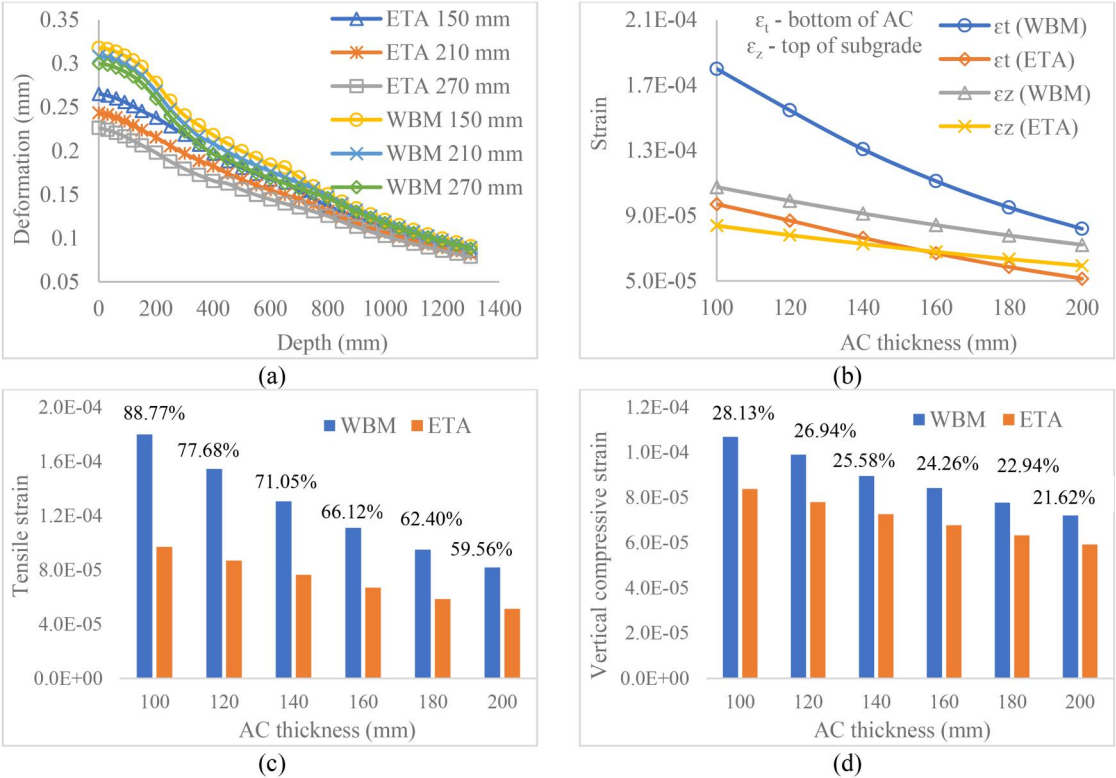


Figure 9. Effect of ETA on (a) maximum deformation, (b) strain, (c) percent change in ϵ_t (bottom of the AC layer), and (d) percent change in ϵ_z (top of the subgrade layer).

Table 13. Effect of ETA on subgrade rutting and asphalt fatigue life.

AC layer thickness (mm)	N_R (msa)		N_f (msa)	
	WBM	ETA	WBM	ETA
100	695	2369	18	407
120	1015	3241	28	435
140	1482	4479	46	539
160	2146	5956	74	720
180	3096	8164	119	996
200	4407	11,274	188	1395

Table 14. Performance of stabilized base (ETA) with varying AC layer thickness.

AC thickness with WBM	AC thickness with ETA	ϵ_t (micro-strains)		ϵ_z (micro-strains)		Reduction in AC thickness
		WBM	ETA	WBM	ETA	
160 mm	100 mm	111.20	97.05	84.26	83.90	60 mm
175 mm	120 mm	98.77	87.01	79.40	78.05	55 mm
195 mm	140 mm	85.06	76.41	73.50	72.72	55 mm
215 mm	160 mm	73.61	66.94	68.17	67.81	55 mm
230 mm	180 mm	66.40	58.53	64.53	63.34	50 mm
250 mm	200 mm	58.25	51.38	60.08	59.29	50 mm

The benefits of ETA in improving rutting and fatigue life of asphalt pavement were further used to explore the possibility of reduction in asphalt layer thickness. Considering a fixed layer thickness of conventional base and asphalt layer, ϵ_t and ϵ_z were evaluated. Taking this value of ϵ_t and ϵ_z as reference, new layer thickness of asphalt layer was evaluated in case of ETA used as

Table 15. Potential of stabilized base (ETA) in reducing conventional base layer thickness.

Thickness of WBM	Thickness of ETA	ϵ_t (micro-strains)		ϵ_z (micro-strains)		Reduction in AC thickness
		WBM	ETA	WBM	ETA	
210 mm	150 mm	120.10	74.61	105.70	103.60	60 mm
230 mm	160 mm	119.90	73.92	101.10	100.50	70 mm
250 mm	175 mm	119.80	72.98	96.74	96.03	75 mm
270 mm	190 mm	119.60	72.20	92.67	91.88	80 mm
290 mm	205 mm	119.50	71.56	88.84	87.99	85 mm
310 mm	220 mm	119.40	71.01	85.22	84.34	90 mm

stabilized base layer. Table 14 shows the possible reduction in asphalt layer thickness whereas Table 15 provides possible reduction in conventional base layer thickness with the use of ETA as stabilized base.

As shown in Table 14, it was found that if ETA is used as the stabilized layer, it may help in the reduction of the top layer thickness without compromising the performance of the whole structure. For example, by limiting ϵ_z value to 85 microstrains for both cases (with ETA and without ETA) the required thickness of the AC layer is reduced by 60 mm (from 160 mm to 100 mm). Considering the practical design point of view, minimum thickness of the asphalt layer should be 80 to 115 mm which includes a minimum thickness of 50 to 75 mm of binder course and 30 to 40 mm of BC-2 as surface course (MoRTH 2013). So, a minimum of 100 mm of asphalt layer thickness can be considered in the pavement design. Parametric analyses of possible thickness reductions in the AC layer for different conditions (ϵ_z and ϵ_t) are given in Table 14 which can help pavement designers for adequate design thickness choices. The results are obtained only considering these two criteria and a standard set of input conditions for an ideal pavement section (see Section 4.4); hence, further investigation should be done before using them in practice.

Keeping the asphalt layer thickness constant (150 mm), potential of emulsion stabilization in reducing the base layer thickness was investigated as shown in Table 15. It was found that for the similar performance in rutting, ETA can be used with 28.57 to 30.43% reduced thickness as compared to conventional unbound base layer. This is important to note that even with this reduced thickness, ETA provides far better performance in asphalt fatigue than conventional unbound base. Similar findings have been reported by Andrews, Radhakrishnan, Koshy, and Prasad (2023) who concluded, ETA as base layer could help in reducing the need of virgin aggregates by 35 to 40%.

As discussed above, ETA has significant potential to improve rutting and fatigue life of asphalt pavement. However, it is important to study the effect of ETA on the stabilized base layer itself as compared to conventional base. Since, addition of bitumen emulsion and cement increases stiffness of the material and may result in higher horizontal tensile strain at the bottom of ETA base layer. It should be noted that unbound granular base will not experience fatigue. However, tensile strain at the bottom of unbound granular base layer has evaluated for comparison with stabilized base layer only. To study the effect of stabilization on ETA layer itself as compared to conventional base, load was varied from 20 to 40 kN and ϵ_t and ϵ_z at the bottom of base layer was noted as shown in Fig. 10.

It was observed that, emulsion treated stabilized base reduces ϵ_t significantly in asphalt layer (see Fig. 9b), however, there is almost no change in ϵ_t value in stabilized base layer as compared to conventional base subjected to different loading conditions (see Fig. 10a). ETA was found more effective in improving rutting life of the base layer, as ϵ_z at the bottom of base layer was found lesser (average reduction is 10.82%) than in case of conventional base (see Fig. 10b).

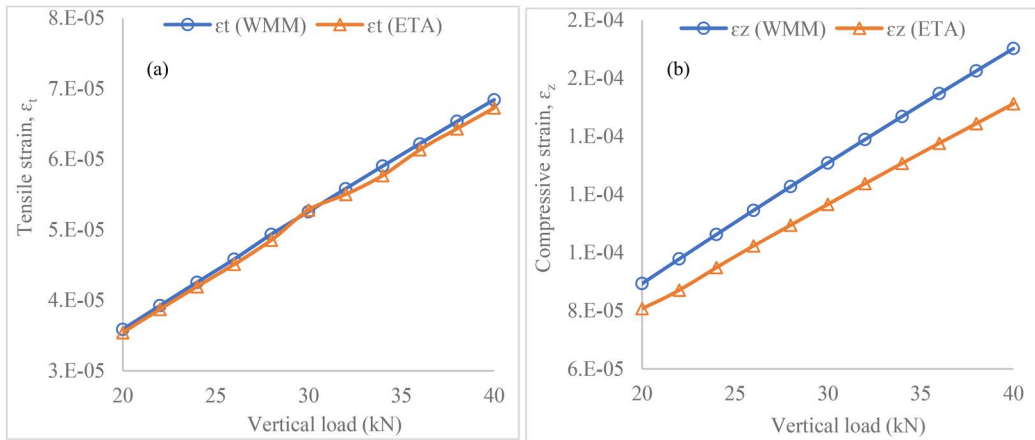


Figure 10. Effect of loading on (a) ϵ_t (at $z = 450$ mm) and (b) ϵ_z (at $z = 450$ mm) in conventional and stabilized base layer.

Table 16. Effect of ETA on pavement performance and overloading allowances.

Base	Thickness (mm)	Load (kN)	ϵ_z (micro-strain) - top of the subgrade layer	N_R (msa)	ϵ_t (micro-strain) - bottom of the AC layer	N_f (msa)
WBM	300	40	172.8	1610	175.6	52
ETA	300	51	172.2	1636	96.8	534
WBM	250	40	192.1	996	176.2	52
ETA	250	50	192.0	999	98.9	492
WBM	200	40	214.6	603	177.1	51
ETA	200	48	211.7	641	101.8	440
WBM	150	40	241.0	356	178.1	50
ETA	150	47	240.5	359	108.0	350

5.2.2. Potential of emulsion stabilized base in providing overloading leverage

Overloading is a major concern in many of the developing nations including India and causes significant damage to AC pavement. It was found that an AC pavement which is generally designed for 15 years when subjected to 5% of overloading, the design life is reduced by 2.7 years (Pais, Amorim, and Minhoto 2013). Due consideration in the design phase itself is needed to take care of overloading-related pavement damage. Structural safety of the pavement against overloading can be ensured by increasing the layer thicknesses or improving the stiffness of existing layers. The focus of the previous section was to evaluate the potential reduction in the thickness of the AC layer with the use of the ETA layer, this section considers the scenario where instead of changing the AC layer thickness, various overloading situation is analyzed. On the tire body (see Fig. 3), the vertical load was increased keeping all other parameters the same as given in Table 16.

To have an easier interpretation of the results, keeping 40 kN with the WBM layer as a reference case, the simulations were repeated with ETA pavement structure until equivalent load resulting in similar strains were found, as shown in Table 16. In terms of benefits, pavements built with an ETA base provided 11 kN to 7 kN leverage depending on the thickness of the ETA considered. Corresponding benefits in N_R and N_f values for different loading combinations are also presented in the same table.

6. Conclusions

This article presents a three-dimensional FE-based framework to study the effect of base stabilization (using ETA) on the structural response as compared to traditional base layer pavement system. In the proposed model, a realistic flexible tire body, flexible pavement structure, and their interactions were considered. Whereas, important input material parameters of the models were obtained from the laboratory tests (mainly ITS and M_r tests), operating parameters such as tire-load were obtained from specifications. At first, simulations were carried for standard set of operating conditions to obtain reference data. In the second stage, parametric analysis with varying input parameters (such as tire-load, thickness layer etc.) were done to study the potential benefits of strengthening ETA layer on overloading leverages or reduction of the thickness for an equivalent response. Using the pavement response data, performance predictions of fatigue lifetime and rutting resistance were obtained (see [Tables 10](#) and [12](#)). Based on all the simulation done in this research, the following conclusions can be drawn:

1. Effect of loading on standard pavement (using WBM as base layer) response was obtained using proposed FE based framework. It was found that change in load affects subgrade rutting and fatigue life of AC layer significantly with the former being more sensitive to change in loading.
2. The effect of temperature on various AC mixes were obtained using M_r test and it was found that, the M_r of mixes is sensitive to change in temperature (a rise in temperature from 25 to 35 °C, reduces M_r by 33 to 41% depending on type of mix). Also, using a standard pavement system, a significant effect on subgrade rutting and fatigue life of the AC layer was observed with later being more sensitive to change in temperature.
3. The proposed FE model was used to study the improvement of pavement performance after replacing the traditional base layer with ETA in base layer stabilization. Based on the findings of critical strains (tensile and compressive) and performance models, it was concluded that, ETA improves the rut resistance and fatigue life of the pavement considerably. The findings of pavement response utilizing ETA as a stabilized base with different trial thicknesses of the AC layer suggests that ETA has huge potential in reducing the asphalt layer thickness. It can also reduce the need of virgin aggregate in base layer by 28.57 to 30.43%.
4. The analyses show that the ETA base layer can be an effective way to compensate for the overlading to an extent. The extent with which the potential leverage is obtained for different design choices are summarized in [Table 16](#).

Future recommendations

In future, the proposed FE model could be validated against field data. The proposed design could also be tested by using accelerated pavement testing facilities and field trials can be done. Further, the proposed FE based framework can be utilized to develop a detailed design guideline. In terms of enhancement of the model, viscoelastic material properties of asphalt mixes and non-linear stress dependent behavior of granular materials can be obtained to simulate more realistic field response of the pavement materials.

Acknowledgment

The authors would like to thank the Ministry of Education, Government of India for providing scholarship to Mr. Abhinav Kumar to support the research reported in this article, as well as GR Infraprojects Limited for supporting the Road Research Laboratory at the IIT (BHU), Varanasi.

Authors contributions

Abhinav Kumar: Conceptualization, Writing – Original Draft, Data Curation, Methodology, Investigation, Visualization, Software, Ankit Gupta: Conceptualization, Conceptualization, Supervision, Methodology, Writing – Review and Editing, Resources, Kumar Anupam: Supervision, Methodology, Writing – Review and Editing, Aakash Singh: Methodology, Data curation, Writing – Original draft, Saranga Premarathna: Software, Writing – Review and Editing.

Disclosure statement

No potential conflict of interest was reported by the author(s).

Funding

The authors declare that they have no financial or personal relationships that may be construed as having impacted the work presented in this study.

Data availability statement

The authors confirm that the supporting data for this study's conclusion are included in the manuscript.

References

- Abadin, M. J., and K. Hayano. 2022. "Investigation of Premature Failure Mechanism in Pavement Overlay of National Highway of Bangladesh." *Construction and Building Materials* 318: 126194. <https://doi.org/10.1016/j.conbuildmat.2021.126194>
- Akarsh, P. K., G. O. Ganesh, S. Marathe, and R. Rai. 2022. "Incorporation of Sugarcane Bagasse Ash to Investigate the Mechanical Behavior of Stone Mastic Asphalt." *Construction and Building Materials* 353: 129089. <https://doi.org/10.1016/j.conbuildmat.2022.129089>
- Andrews, J. K., V. Radhakrishnan, R. Z. Koshy, V. Chowdary, and T. K. Subhash. 2023. "Field Investigation of Material Layer Properties for Emulsion-Treated Base Layer Application in Low-Volume Roads." *International Journal of Pavement Engineering* 24 (1): 2190117. <https://doi.org/10.1080/10298436.2023.2190117>
- Andrews, J. K., V. Radhakrishnan, R. Z. Koshy, and C. S. R. K. Prasad. 2023. "Construction and Evaluation of Low-Volume Roads Incorporating Emulsion Treated Base Layers." *Indian Geotechnical Journal* 53 (5): 1041–1052. <https://doi.org/10.1007/s40098-023-00724-5>
- Anupam, K., D. Akinmade, C. Kasbergen, S. Erkens, and F. Adebisi. 2023. "A State-of-the-Art Review of Natural Bitumen in Pavement: Underlining Challenges and the Way Forward." *Journal of Cleaner Production* 382: 134957. <https://doi.org/10.1016/j.jclepro.2022.134957>
- Anupam, K., T. Tang, C. Kasbergen, A. Scarpas, and S. Erkens. 2021. "3-D Thermomechanical Tire–Pavement Interaction Model for Evaluation of Pavement Skid Resistance." *Transportation Research Record* 2675 (3): 65–80. <https://doi.org/10.1177/0361198120963101>
- Asphalt Mix Design Manual for South Africa. 2002. Southern African Bitumen Association (Sabita), Cape Town, South Africa.
- ASTM D 4123. 1995. *Standard Test Method for Indirect Tension Test for Resilient Modulus of Bituminous Mixtures*. ASTM International, West Conshohocken, PA.
- ASTM D 6373. 1999. *Standard Specification for Performance-Graded Asphalt Binder*. ASTM International, West Conshohocken, PA.
- ASTM D 6931. 2017a. *Standard Test Method for Indirect Tensile (IDT) Strength of Asphalt Mixtures*. American Society for Testing and Materials, West Conshohocken, PA.
- ASTM D 6931. 2017b. *Standard Test Method for Indirect Tensile (IDT) Strength of Bituminous Mixtures 1*. American Society for Testing and Materials, West Conshohocken, PA. <https://doi.org/10.1520/D6931-17.2>
- ASTM D 7369. 2011. *Standard Test Method for Determining the Resilient Modulus of Bituminous Mixtures by Indirect Tension Test*. West Conshohocken, PA: ASTM International.
- Baghini, M. S., A. B. Ismail, M. R. B. Karim, F. Shokri, and A. A. Firoozi. 2017. "Effects on Engineering Properties of Cement-Treated Road Base with Slow Setting Bitumen Emulsion." *International Journal of Pavement Engineering* 18 (3): 202–215. <https://doi.org/10.1080/10298436.2015.1065988>

- Bocci, M., F. Canestrari, A. Grilli, E. Pasquini, and D. Lioi. 2010. "Recycling Techniques and Environmental Issues Relating to the Widening of an High Traffic Volume Italian Motorway." *International Journal of Pavement Research and Technology* 3 (4): 171.
- Chehelgo, K., Z. C. Abiero Gariy, and S. Muse Shitote. 2018. "Laboratory Mix Design of Cold Bitumen Emulsion Mixtures Incorporating Reclaimed Asphalt and Virgin Aggregates." *Buildings* 8 (12): 177. <https://doi.org/10.3390/buildings8120177>
- Chhabra, R. S., G. D. R. RN, and S. K. Singh. 2022. "Effectiveness of Liquid Antistripping Additive for Emulsion-Treated Base Layer Using Reclaimed Asphalt Pavement Material." *Advances in Civil Engineering* 2022 (1): 6280681. <https://doi.org/10.1155/2022/6280681>
- De Beer, M., and J. E. Grobler. 1994. "Towards Improved Structural Design Criteria for Granular Emulsion Mixes (GEMS)." Paper presented at Proceedings of the 6th Conference on Asphalt Pavements for Southern Africa, Capsa'94, Held Cape Town, October 1994. vol 1.
- De Beer, M., C. Fisher, and F. J. Jooste. 2002. "Evaluation of Non-Uniform Tyre Contact Stresses on Thin Asphalt Pavements." In *Ninth International Conference on Asphalt Pavements, ISAP*, Copenhagen, Denmark. Vol. 5, 19–22.
- Dias, C. R. C., W. P. Núñez, L. A. T. Brito, M. G. Johnston, J. A. P. Ceratti, L. L. Wagner, and W. Fedrigo. 2023. "Bitumen Stabilized Materials as Pavement Overlay: Laboratory and Field Study." *Construction and Building Materials* 369: 130562. <https://doi.org/10.1016/j.conbuildmat.2023.130562>
- Dias, C. R. C., W. P. Núñez, and W. Fedrigo. 2024. "A Bitumen-Stabilized Base Course as a Pavement Overlay Anti-Reflective Cracking Solution." In *International Symposium on Asphalt Pavement & Environment*, 401–406. Cham, Switzerland: Springer Nature.
- Dwyer-Joyce, R. S., and B. W. Drinkwater. 2003. "In Situ Measurement of Contact Area and Pressure Distribution in Machine Elements." *Tribology Letters* 14 (1): 41–52. <https://doi.org/10.1023/A:1021766216019>
- Ghosh, A., A. Padmarekha, and J. M. Krishnan. 2013. "Implementation and Proof-Checking of Mechanistic-Empirical Pavement Design for Indian Highways Using AASHTOWare Pavement ME Design Software." *Procedia-Social and Behavioral Sciences* 104: 119–128. <https://doi.org/10.1016/j.sbspro.2013.11.104>
- Grilli, A., A. Graziani, E. Bocci, and M. Bocci. 2016. "Volumetric Properties and Influence of Water Content on the Compactability of Cold Recycled Mixtures." *Materials and Structures* 49 (10): 4349–4362. <https://doi.org/10.1617/s11527-016-0792-x>
- Gupta, A., P. Kumar, and R. Rastogi. 2015. "Critical Pavement Response Analysis of Low-Volume Pavements Considering Nonlinear Behavior of Materials." *Transportation Research Record* 2474 (1): 3–11. <https://doi.org/10.3141/2474-01>
- Gupta, A., S. K. Pradhan, L. Bajpai, and V. Jain. 2021. "Numerical Analysis of Rubber Tire/Rail Contact Behavior in Road Cum Rail Vehicle under Different Inflation Pressure Values Using Finite Element Method." *Materials Today: Proceedings* 47: 6628–6635. <https://doi.org/10.1016/j.matpr.2021.05.100>
- Helwany, S., J. Dyer, and J. Leidy. 1998. "Finite-Element Analyses of Flexible Pavements." *Journal of Transportation Engineering* 124 (5): 491–499. [https://doi.org/10.1061/\(ASCE\)0733-947X\(1998\)124:5\(491\)](https://doi.org/10.1061/(ASCE)0733-947X(1998)124:5(491)).
- Hossain, M., and P. Steinmann. 2013. "More Hyperelastic Models for Rubber-like Materials: Consistent Tangent Operators and Comparative Study." *Journal of the Mechanical Behavior of Materials* 22 (1-2): 27–50. <https://doi.org/10.1515/jmbm-2012-0007>
- IRC 111. 2009. *Specifications for Dense Graded Bituminous Mixes*. Indian Road Congress, New Delhi, India.
- IRC 37-2012. 2012. *Guidelines for the Design of Flexible Pavements (Third Revision)*. Indian Road Congress, New Delhi, India.
- IRC 37-2018. 2018. *Guidelines for the Design of Flexible Pavements (Fourth Revision)*. Indian Road Congress, New Delhi, India.
- IRC-SP-135. 2022. *Manual for the Design of Hot Bituminous Mixes*. Indian Road Congress, New Delhi, India.
- IS 73. 2013. *Paving Bitumen – Specification*. New Delhi, India: Bureau of Indian Standards.
- IS 1203. 2022. *Methods for Testing Tar and Bituminous Materials—Determination of Penetration*. New Delhi, India: Bureau of Indian Standards.
- IS 1205. 1978. *Methods for Testing Tar and Bituminous Materials, Softening Point Test*. New Delhi, India: Bureau of Indian Standards.
- IS 1206. 1978. *Methods for Testing Tar and Bituminous Materials, Viscosity Test*. New Delhi, India: Bureau of Indian Standards.
- IS 2386-1. 1963. *Methods of Test for Aggregates for Concrete, Part I: Particle Size and Shape*. New Delhi, India: Bureau of Indian Standards.
- IS 2386-4. 1963. *Methods of Test for Aggregates for Concrete, Part 4: Mechanical Properties*. New Delhi, India: Bureau of Indian Standards.
- IS 2720 – Part 8. 1994. *Determination of Water Content-Dry Density Relation Using Heavy Compaction*. New Delhi, India: Bureau of Indian Standards.
- IS 2720 – Part 40. 1997. *Determination of Free Swell Index of Soils*. New Delhi, India: Bureau of Indian Standards.

- IS 8887. 2004. *Bitumen Emulsion for Roads (Cationic Type)-Specification (Second Revision)*. New Delhi, India: Bureau of Indian Standards.
- Jiang, X., C. Zeng, X. Gao, Z. Liu, and Y. Qiu. 2019. "3D FEM Analysis of Flexible Base Asphalt Pavement Structure under Non-Uniform Tyre Contact Pressure." *International Journal of Pavement Engineering* 20 (9): 999–1011. <https://doi.org/10.1080/10298436.2017.1380803>
- Júnior, C. L. D. S. R., L. A. T. Brito, L. F. Heller, G. G. Schreinert, W. P. Núñez, J. A. P. Ceratti, and C. Merighi. 2020. "Impact on Pavement Deterioration Due to Overload Vehicle Regulation in Brazil." *Transportation Research Procedia* 45: 842–849. <https://doi.org/10.1016/j.trpro.2020.02.085>
- Karami, M., H. Nikraz, S. Sebayang, and L. Irianti. 2018. "Laboratory Experiment on Resilient Modulus of BRA Modified Asphalt Mixtures." *International Journal of Pavement Research and Technology* 11 (1): 38–46. <https://doi.org/10.1016/j.ijprt.2017.08.005>
- Khan, S., M. N. Nagabhushana, D. Tiwari, and P. K. Jain. 2013. "Rutting in Flexible Pavement: An Approach of Evaluation with Accelerated Pavement Testing Facility." *Procedia-Social and Behavioral Sciences* 104: 149–157. <https://doi.org/10.1016/j.sbspro.2013.11.107>
- Kumar, A., A. Gupta, K. Anupam, and V. P. Wagh. 2024. "Finite Element-Based Framework to Study the Response of Bituminous Concrete Pavements under Different Conditions." *Construction and Building Materials* 417: 135368. <https://doi.org/10.1016/j.conbuildmat.2024.135368>
- Kumar, A., T. Tang, A. Gupta, and K. Anupam. 2023. "A State-of-the-Art Review of Measurement and Modelling of Skid Resistance: The Perspective of Developing Nation." *Case Studies in Construction Materials* 18: E 02126. <https://doi.org/10.1016/j.cscm.2023.e02126>
- Li, Y., W. Y. Liu, and S. Frimpong. 2012. "Effect of Ambient Temperature on Stress, Deformation and Temperature of Dump Truck Tire." *Engineering Failure Analysis* 23: 55–62. <https://doi.org/10.1016/j.engfailanal.2012.02.004>
- Lu, G., C. Wang, P. Liu, S. Pyrek, M. Oeser, and S. Leischner. 2019. "Comparison of Mechanical Responses of Asphalt Mixtures under Uniform and Non-Uniform Loads Using Microscale Finite Element Simulation." *Materials* 12 (19): 3058. <https://doi.org/10.3390/ma12193058>
- Mittal, A., K. Arora, G. Kumar, and P. K. Jain. 2018. "Comparative Studies on Performance of Bituminous Mixes Containing Laboratory Developed Hard Grade Bitumen." *Advances in Civil Engineering Materials* 7 (2): 92–104. <https://doi.org/10.1520/ACEM20170039>
- MoRTH. 2013. *Specifications for Road and Bridge Work (Fifth Revision)*. Indian Road Congress, New Delhi, India.
- Munoz, J. S. C., F. Kaseer, E. Arambula, and A. E. Martin. 2015. "Use of the Resilient Modulus Test to Characterize Asphalt Mixtures with Recycled Materials and Recycling Agents." *Transportation Research Record* 2506 (1): 45–53. <https://doi.org/10.3141/2506-05>
- Nasimifar, M., S. Thyagarajan, and N. Sivaneshwaran. 2017. "Backcalculation of Flexible Pavement Layer Moduli from Traffic Speed Deflectometer Data." *Transportation Research Record* 2641 (1): 66–74. <https://doi.org/10.3141/2641-09>
- Oubahdou, Y., E. R. Wallace, P. Reynaud, B. Picoux, J. Dopeux, C. Petit, and D. Nélias. 2021. "Effect of the Tire–Pavement Contact at the Surface Layer When the Tire Is Tilted in Bend." *Construction and Building Materials* 305: 124765. <https://doi.org/10.1016/j.conbuildmat.2021.124765>
- Pais, J. C., S. I. Amorim, and M. J. Minhoto. 2013. "Impact of Traffic Overload on Road Pavement Performance." *Journal of Transportation Engineering* 139 (9): 873–879. [https://doi.org/10.1061/\(ASCE\)TE.1943-5436.0000571](https://doi.org/10.1061/(ASCE)TE.1943-5436.0000571)
- Pan, Q. X., C. C. Zheng, S. T. Lü, G. P. Qian, J. H. Zhang, P. H. Wen, B. C. Milkos, and H. D. Zhou. 2021. "Field Measurement of Strain Response for Typical Asphalt Pavement." *Journal of Central South University* 28 (2): 618–632. <https://doi.org/10.1007/s11771-021-4626-9>
- Pérez, I., L. Medina, and M. Á. del Val. 2013. "Mechanical Properties and Behaviour of in Situ Materials Which Are Stabilised with Bitumen Emulsion." *Road Materials and Pavement Design* 14 (2): 221–238. <https://doi.org/10.1080/14680629.2013.779301>
- Phromjan, J., and C. Suvanjumrat. 2018. "A Suitable Constitutive Model for Solid Tire Analysis under Quasi-Static Loads Using Finite Element Method." *Engineering Journal* 22 (2): 141–155. <https://doi.org/10.4186/ej.2018.22.2.141>
- Premarathna, W. A. A. S., J. A. S. C. Jayasinghe, K. K. Wijesundara, R. R. M. S. K. Ranatunga, and C. D. Senanayake. 2020. "Performance Comparison of Solid Tires and Non-Pneumatic Tires Using Finite Element Method: Application to Military Vehicles." *Holistic Approach to National Growth and Security*, 13th International Research Conference, General Sir John Kotelawala Defence University, Sri Lanka. 120–128.
- Premarathna, W. A. A. S., J. A. S. C. Jayasinghe, K. K. Wijesundara, P. Gamage, R. R. M. S. K. Ranatunga, and C. D. Senanayake. 2021. "Investigation of Design and Performance Improvements on Solid Resilient Tires through Numerical Simulation." *Engineering Failure Analysis* 128: 105618. <https://doi.org/10.1016/j.engfailanal.2021.105618>
- Ranadive, M. S., and A. B. Tapase. 2016. "Parameter Sensitive Analysis of Flexible Pavement." *International Journal of Pavement Research and Technology* 9 (6): 466–472. <https://doi.org/10.1016/j.ijprt.2016.12.001>

- Shoop, S. A. 2001. *Finite Element Modeling of Tire-Terrain Interaction*. University of Michigan, East Lansing, Michigan, United States.
- Shukla, M. K., A. Walia, V. Purohit, V. Vyas, and G. Singh. 2023. "Establishment of Best Practices for Laboratory Evaluation of Stabilized Base Layers and Comparative Study on Influence of Different Types of Stabilizers." *Construction and Building Materials* 400: 132691. <https://doi.org/10.1016/j.conbuildmat.2023.132691>
- Siddharthan, R. V., N. Krishnamenon, M. El-Mously, and P. E. Sebaaly. 2002. "Investigation of Tire Contact Stress Distributions on Pavement Response." *Journal of Transportation Engineering* 128 (2): 136–144. <https://doi.org/10.1061/ASCE0733-947X2002128:2136>
- Singh, A., A. Behl, and A. Dhamaniya. 2022. "Feasibility Study on the Use of Multilayer Plastic (MLP) Waste in the Construction of Asphalt Pavements." In *International Conference on Trends and Recent Advances in Civil Engineering*, 207–226. Singapore: Springer Nature.
- Singh, A., and A. Gupta. 2024. "Mechanical and Economical Feasibility of LDPE Waste-Modified Asphalt Mixtures: Pathway to Sustainable Road Construction." *Scientific Reports* 14 (1): 25311. <https://doi.org/10.1038/s41598-024-75196-5>
- Singh, A., A. Gupta, and M. Miljković. 2023. "Intermediate-and High-Temperature Damage of Bitumen Modified by HDPE from Various Sources." *Road Materials and Pavement Design* 24 (sup1): 640–653. <https://doi.org/10.1080/14680629.2023.2181017>
- Usman, N., and M. I. M. Masirin. 2019. "Performance of Asphalt Concrete with Plastic Fibres." In *Use of Recycled Plastics in Eco-Efficient Concrete*, 427–440. Elsevier. <https://doi.org/10.1016/B978-0-08-102676-2.00020-7>
- Venudharan, V., and K. P. Biligiri. 2015. "Estimation of Phase Angles of Asphalt Mixtures Using Resilient Modulus Test." *Construction and Building Materials* 82: 274–286. <https://doi.org/10.1016/j.conbuildmat.2015.02.061>
- Wang, H., and I. L. Al-Qadi. 2010. "Near-Surface Pavement Failure under Multiaxial Stress State in Thick Asphalt Pavement." *Transportation Research Record* 2154 (1): 91–99. <https://doi.org/10.3141/2154-08>
- Wang, H., I. L. Al-Qadi, and I. Stanciulescu. 2012. "Simulation of Tyre–Pavement Interaction for Predicting Contact Stresses at Static and Various Rolling Conditions." *International Journal of Pavement Engineering* 13 (4): 310–321. <https://doi.org/10.1080/10298436.2011.565767>
- Yao, K., X. Jiang, J. Jiang, Z. Yang, and Y. Qiu. 2021. "Influence of Modulus of Base Layer on The Strain Distribution for Asphalt Pavement." *The Baltic Journal of Road and Bridge Engineering* 16 (4): 126–152. <https://doi.org/10.7250/bjrbe.2021-16.542>
- Zhang, L., C. Wang, X. Dong, and X. Zhang. 2020. "Structural Response Analysis of Nonlinear Pavement Based on Granular Material." *IOP Conference Series: Materials Science and Engineering* 730 (1): 012018. <https://doi.org/10.1088/1757-899X/730/1/012018>